

1-1-1989

Decoupling and adaptive control and stabilization of two-link elastic robotic arm

Arijit Das

University of Nevada, Las Vegas

Follow this and additional works at: <https://digitalscholarship.unlv.edu/rtds>

Repository Citation

Das, Arijit, "Decoupling and adaptive control and stabilization of two-link elastic robotic arm" (1989). *UNLV Retrospective Theses & Dissertations*. 47.

<http://dx.doi.org/10.25669/o9n5-9tmd>

This Thesis is protected by copyright and/or related rights. It has been brought to you by Digital Scholarship@UNLV with permission from the rights-holder(s). You are free to use this Thesis in any way that is permitted by the copyright and related rights legislation that applies to your use. For other uses you need to obtain permission from the rights-holder(s) directly, unless additional rights are indicated by a Creative Commons license in the record and/or on the work itself.

This Thesis has been accepted for inclusion in UNLV Retrospective Theses & Dissertations by an authorized administrator of Digital Scholarship@UNLV. For more information, please contact digitalscholarship@unlv.edu.

INFORMATION TO USERS

The most advanced technology has been used to photograph and reproduce this manuscript from the microfilm master. UMI films the text directly from the original or copy submitted. Thus, some thesis and dissertation copies are in typewriter face, while others may be from any type of computer printer.

The quality of this reproduction is dependent upon the quality of the copy submitted. Broken or indistinct print, colored or poor quality illustrations and photographs, print bleedthrough, substandard margins, and improper alignment can adversely affect reproduction.

In the unlikely event that the author did not send UMI a complete manuscript and there are missing pages, these will be noted. Also, if unauthorized copyright material had to be removed, a note will indicate the deletion.

Oversize materials (e.g., maps, drawings, charts) are reproduced by sectioning the original, beginning at the upper left-hand corner and continuing from left to right in equal sections with small overlaps. Each original is also photographed in one exposure and is included in reduced form at the back of the book. These are also available as one exposure on a standard 35mm slide or as a 17" x 23" black and white photographic print for an additional charge.

Photographs included in the original manuscript have been reproduced xerographically in this copy. Higher quality 6" x 9" black and white photographic prints are available for any photographs or illustrations appearing in this copy for an additional charge. Contact UMI directly to order.

U·M·I

University Microfilms International
A Bell & Howell Information Company
300 North Zeeb Road, Ann Arbor, MI 48106-1346 USA
313/761-4700 800/521-0600



Order Number 1338255

**Decoupling and adaptive control and stabilization of two-link
elastic robotic arm**

Das, Arijit, M.S.

University of Nevada, Las Vegas, 1989

U·M·I
300 N. Zeeb Rd.
Ann Arbor, MI 48106

**DECOUPLING ¹ AND ADAPTIVE CONTROL AND
STABILIZATION OF TWO LINK ELASTIC ROBOTIC ARM .**

**by
Arijit Das**

**A thesis submitted in partial fulfillment
of the requirements for the degree of**

Master of Science

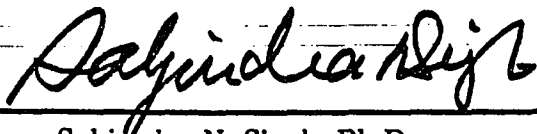
in

Electrical Engineering

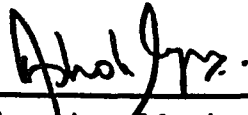
**Department of Computer Science and Electrical Engineering
University of Nevada Las Vegas
August, 1989**

¹This research was supported by the U.S. Army Research Office under ARO Grant No. DAAL03-87-G-0004

The thesis of Arijit Das for the degree of Master of Science
in Electrical Engineering is approved



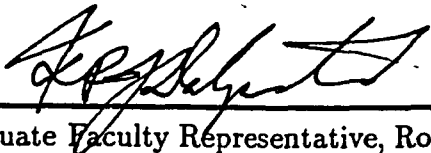
Chairperson, Sahjendra N. Singh, Ph.D.



Examining Committee Member, Ashok Iyer, Ph.D.



Examining Committee Member, Kyoung Il Kim, Ph.D.



Graduate Faculty Representative, Rohan Dalpatadu, Ph.D.



Graduate Dean, Ronald W. Smith, Ph.D.

University of Nevada Las Vegas
August, 1989

Acknowledgement

I would like to thank Dr. S. N. Singh for introducing me to topics in Robotics and Control.

I would also like to thank Dr. Ashok Iyer for making me aware of Robotics research at UNLV, Dr. Wyman for willing to support me during summers through the ARO grant, Dr. K. I. Kim and Dr. R. Dalpatadu for agreeing to be in my thesis defence committee.

I would also like to thank the faculty and staff of the Department of Electrical Engineering and Computer Science for providing me facilities for graduate study.

Finally I would like to thank my parents for their moral support, guidance and constant encouragement all through my education.

Abstract

In this thesis the control and stabilization of a two link flexible robotic arm is considered. Two schemes have been implemented. The first scheme is based on nonlinear inversion, a nonlinear controller is designed for the trajectory control of the joint angles using joint torquers. The inverse controller includes a servocompensator for robustness. Although, the inverse controller accomplishes trajectory control of the joint angles, this excites the elastic modes of the arm. In order to damp the elastic oscillations, a stabilizer is designed for a linearized system about the terminal state using pole assignment technique. A switching logic is used to turn on the stabilizer when it enters a specified neighbourhood. A simplified controller has also been designed neglecting the Coriolis and Centrifugal forces.

In the second scheme the control system design is based on nonlinear adaptive control and linear stabilization. First a nonlinear adaptive control law is derived such that in the closed-loop system the joint-angles are precisely controlled to track reference trajectories. Once the joint angle enters the vicinity of the desired terminal value, a linear stabilizer designed based on a linear model of the arm is switched to accomplish the final capture of the desired state.

Simulation results are presented for all cases to show that in the closed-loop system accurate joint angle trajectory tracking and elastic mode stabilization can be accomplished

inspite of the uncertainty in the payload.

Contents

1	Introduction	1
2	Mathematical Model	7
3	Decoupling Control	10
3.1	Introduction	10
3.2	Problem Formulation	11
3.3	Joint Angle Control By System Inversion	12
3.4	Linear Stabilizer	14
3.5	Simulation Results	18
3.5.1	A. Trajectory Control: Stabilizer Loop Open	20
3.5.2	B. Trajectory control and Stabilization : Nominal System	20
3.5.3	C. Trajectory Control and stabilization : Lower payload	21
3.5.4	D. Trajectory Control and Stabilization: Higher payload	21

3.5.5	E. Trajectory Tracking and Stabilization: Effect of Pole Assignment	22
3.5.6	F. Trajectory Tracking and Stabilization: Slow Command	22
3.6	Conclusion	23
4	Effect of Coriolis and Centrifugal Forces	24
4.1	Introduction	24
4.2	Problem Formulation	25
4.3	Joint Angle Control	26
4.4	Linear Stabilizer	27
4.5	Simulation Results	28
4.5.1	A. Trajectory control and Stabilization : Nominal System	29
4.5.2	B. Trajectory Control and Stabilization: Higher payload	30
4.5.3	C. Trajectory Control and stabilization : Fast System	30
4.6	Conclusions	31
5	Adaptive control	32
5.1	Introduction	32
5.2	Problem Formulation	33
5.3	Adaptive Control of Joint Angles	34
5.4	Linear Stabilizer	38

5.5	Simulation Results	41
5.5.1	A. Trajectory control and Stabilization : Nominal System	42
5.5.2	B. Trajectory Control and stabilization : Lower payload	43
5.5.3	C. Trajectory Control and Stabilization: Higher payload	43
5.6	Conclusion	44
6	Conclusion	45
	Bibliography	46
A	Appendix	70

List of Figures

1	Figure 1. Flexible Robot Arm Model	51
Figures for Dual Mode Inverse system		52
2	Figure 2. The Closed Loop System	51
3	Figure 3. Stabilizer loop open	52
3.1	Joint angles	52
3.2	Elastic deflections	52
4	Figure 4. Nominal payload	53
4.1	Joint angles	53
4.2	Generalized coordinates	53
4.3	Generalized coordinates	54
4.4	Joint angle errors	54
4.5	Elastic deflections	55
4.6	control torques	55

5	Figure 5. Off-nominal Lower Payload	56
5.1	Joint angles	56
5.2	Joint angle errors	56
5.3	Elastic deflection	57
6	Figure 6. Off-nominal higher payload	58
6.1	Joint angle errors	58
6.2	Elastic Deflections	58
6.3	Control torques	59
7	Figure 7. Pole Assignment	60
7.1	Joint angle errors	60
7.2	Elastic deflections	60
7.3	control torques	61
8	Figure 8. Slow Command	62
8.1	Joint angles	62
8.2	Elastic deflections	62

Figures for Approximate controller 63

9	Figure 9. Nominal System	63
9.1	Joint angles	63
9.2	Elastic deflections	63
10	Figure 10. Higher payload	64

10.1	Elastic deflections	64
10.2	Joint angle errors	64
11	Figure 11. Fast System	65
11.1	Elastic deflection	65
11.2	Joint angle errors	65
Figures for Adaptive System		66
12	Figure 12. Closed loop system	66
13	Figure 13. Nominal system	67
13.1	Joint angles	67
13.2	Elastic deflections	67
14	Figure 14. Lower payload	68
14.1	Elastic deflections	68
14.2	Joint angle errors	68
15	Figure 15. Higher payload	69
15.1	Elastic deflections	69
15.2	Joint angle errors	69

Chapter 1

Introduction

The design of light weight robotic manipulators is of considerable interest. Use of such manipulators results in higher speed of operation, less overall cost, less energy consumption, smaller actuator size, higher productivity, etc. However, light weight manipulators have considerable structural flexibility. Dynamics of elastic manipulators is governed by coupled highly nonlinear differential and partial differential equations. Control of such manipulators is a complicated problem. Furthermore, since the robots must handle a wide variety of payloads along given paths, robustness of the control system becomes very important.

Recently, some attempt has been made to treat the question of control of robotic systems having elastic links [1- 7] using linearized models for small maneuvers. In [1] the author has designed a compensation for the linearized model and has tried to verify by simulation how good the approach is when applied to the nonlinear system. In [6] an integral plus state feedback is designed based on a linearized model of the robot arm. In [7] a Linear Quadratic Control with a prescribed degree of stability has been used. For the control of a nonlinear elastic arm having two rigid links and one elastic link, controllers based on nonlinear

invertibility of related input-output maps and linear stabilization have been designed in [9-10]. In [10] the derived control law includes terms to compensate for the elastic motion of the arm and the control forces acting at the tip of the beam. Experimental results on the end-point control of a flexible one-link robotic arm has been presented in [11- 12]. In [11] a control algorithm using Linear Quadratic Gaussian approach has been designed. A nonlinear controller for an elastic arm in the presence of uncertainty has been designed in [13]. The control law in [13] asymptotically decouples the elastic dynamics of the robotic arm from the rigid ones and allows the force controller to be designed separately using the feedback of elastic modes for vibration stabilization. A similar approach will be used in this study.

In this thesis, we consider the control of a two-link elastic arm which is designed in [1-2]. The equations of motion of a system of two flexible beams pinned at one end at the joint has been derived by the author of [1]. He has applied Lagrange's equation applied to the distributed system. Basically he has obtained the model by superimposing the flexible motion over a hypothetical rigid body motion. However, it may be pointed out that the approach just mentioned is applicable to multi-link flexible manipulators and also to slewing of elastic space systems. The elastic arm of this thesis, has two rotational joints and two joint torquers have been provided for the control of the links.

As can be realized the open loop system is nonlinear and oscillatory due to inherent vibration modes of the flexible links. There are a large order of modes. The vibration of the system introduces additional difficulties into the control problem. Moreover, there

exists uncertainty in the system due to payload changes, joint frictional forces, etc. The contribution of this thesis lies in the development of nonlinear control laws for joint angle control and the design of linear feedback laws for stabilization of the complete elastic robotic arm.

First, a nonlinear decoupling control is derived for controlling the joint angles based on the inversion of the input (joint torques)-output (joint angles) map of the robotic arm. For the inversion of the map, the output variables are differentiated and in the resulting equation the nonlinear interacting terms are cancelled out by the proper choice of the control torques. Furthermore, PID (Proportional Integral and Derivative) terms as functions of the joint angle tracking errors are included in the control law for obtaining third order linear dynamics for each tracking error. the integral term in the control law is introduced to obtain robustness in the system. Interestingly, the decoupling nonlinear controller accomplishes robust joint angle tracking and asymptotically linearizes the system as the joint angular velocity converges to zero. The control of joint angles excites the elastic modes of the links and it becomes necessary to damp the vibration of the links by using auxillary control signal. The complete closed-system is simulated on the digital computer. The system responses are obtained in the context of nominal system, payload uncertainty, and speed of trajectory following.

To dampen the vibrations we use a stabilizer. The design of the stabilizer is based on linear control theory. We linearize the system about the terminal point. Then using pole placement technique we move the poles of the open loop system to obtain a stable system.

The complete algorithm is implemented in CTRL-C, a linear systems design interactive software package. The feedback gains thus obtained are used to stabilize the system. When the robot arm has reached close to the terminal position, we switch on the stabilizer. The switching is automatic and based on how close the arm is to the terminal state. The stabilizer acting along with a linearized version of the decoupling control will bring the robot arm to rest at its terminal position. Simulation of the system with respect to pole placement of the stabilizer was also done.

The synthesis of the controller in [8] used to achieve joint angle control, requires a large amount of computation inherent in the inverse controller which may prohibit real-time implementation of the controller. So the question of simplification of control law by neglecting Coriolis and Centrifugal forces is considered. These terms that are being neglected are second order terms in velocity. So we expect the simplified controller to perform close to the complete controller during slow motion, but that may not be the case during fast motion. So the adverse effect of this simplification on the performance is examined. Selected responses of [8] have been presented in [29]. The simplified controller was simulated with respect to the nominal system, payload uncertainty and speed of trajectory following. The results are compared with that of the complete controller.

Adaptive control of a linear elastic robotic systems also have been considered in literature [12, 19, 20, 21, 22]. A variable structure control system for two-link flexible arm has been designed in [23]. A nonlinear adaptive control scheme has been presented in [13] which uses additional actuators on the elastic link for stabilization. Control of flexible joint

robotic systems with uncertainty also has been considered in [24, 25, 26].

The decoupling control laws require the complete knowledge of the system dynamics. Since the computation of these terms is complicated, (moreover uncertainty also exists) one would like to design a controller which does not require any information on the system, dynamics. We take such an adaptive approach for joint angle control in this thesis. We design a nonlinear adaptive controller for joint angle trajectory tracking. This adaptive scheme does not require any information on the uncertainty bound and includes a dynamic system in the feedback path. The control signal is a function of only tracking error and its derivatives. The derivation of this control is based on the results of [27]. We note that although adaptive controller can control the joint angles, it excites the link vibration during maneuver. For the stabilization of elastic modes, a stabilizer is designed.

The design of the stabilizer is a little different in this case. We linearize the system and design the stabilizer using pole placement technique. The time to switch the stabilizer is no longer automatic. The stabilizer is expected to work best when the robot arm has reached close to the terminal state. When the stabilizer is turned on we do not have a linearized version of the adaptive controller. In fact the adaptive controller is completely switched off. We have calculated the control needed to hold joint angle of the robotic arm at the terminal state. So this is applied along with the stabilizer control. Extensive simulation will be done to verify the results in relation to payload uncertainty.

The organization of this thesis is as follows. Chapter 2 describes the Mathematical Model. Chapter 3 is about the Nonlinear Decoupling control scheme. Chapter 4 considers

a simplified version of the controller described in chapter 3. Finally chapter 5 discusses the adaptive control law.

Chapter 2

Mathematical Model

A robotic arm with two revolute joints, is shown in Fig 1. The system is composed of two flexible bodies connected by a frictionless pinned joint. One end of the system is assumed to have planar motion and the relative motion of the two bodies results from torques applied at each joint of the system. In order to facilitate the description, the joints are numbered 1 and 2 and the bodies will be represented by two flexible beams. At the end of beam 1, a concentrated mass representing the servo-motor is present at joint 2 and the joint itself; at the end of beam 2, a discrete mass can also appear, representing a payload to be moved between two points in the plane.

In Fig 1., OXY is an inertial reference frame with origin at joint 1, Ox_1y_1 is a reference frame with origin at joint 1, axis x_1 is tangent to link 1 at point O , and $O_2x_2y_2$ is a reference frame with origin at joint 2 with its axis x_2 tangent to link 2 at point O_2 . The axis OX points vertically down. If the links were undeformed, the arm would lie along OO_1O_3 . Let θ_1 , and θ_2 denote the rotation angles of this hypothetical rigid arm. The elastic deflection of the manipulator is denoted by $u_{e1}(x_1, t)$ for link 1 and $u_{e2}(x_2, t)$ for link 2 and these deflections

in the deformed links may be represented by

$$\begin{aligned} u_{e1}(x_1, t) &= \sum_{i=1}^n \phi_{1i}(x_1) q_{1i}(t) \\ u_{e2}(x_2, t) &= \sum_{i=1}^n \phi_{2i}(x_2) q_{2i}(t) \end{aligned} \quad (2.1)$$

where ϕ_{1i} and ϕ_{2i} , $i=1, \dots, n$, is a set of appropriately chosen basis functions; q_{kj} , $k = 1, 2, j = 1, \dots, n$, are the time dependent generalized coordinates; and x_1 and x_2 denote the distances from joint 1 and joint 2 along OO_1 and O_2O_3 , respectively. Here, we neglect the longitudinal and torsional modes and it is assumed that the elastic deformation is small. In this study similar to [1, 2, 12], we select the basis functions ϕ_{ij} as the eigenfunctions of a cantilever beam. It has been found by experimentation that the cantilever eigenfunctions form an excellent basis for a compliant link in a dynamic situation [12]. Thus the motion of the arm is completely described by the vector of generalized coordinates $z = (\theta_1, \theta_2, q_{11}, \dots, q_{1n}, q_{21}, \dots, q_{2n})^T \in R^{2(n+1)}$ (Here T denotes transposition).

Equations of motion of the arm are derived using Lagrangian approach. For this purpose, first the kinetic energy, K and the potential energy, V are obtained. Then equations of motion are given by

$$\frac{d}{dt} \left(\frac{\partial K}{\partial \dot{z}} \right) - \frac{\partial K}{\partial z} + \frac{\partial V}{\partial z} = B_1 u \quad (2.2)$$

where $u = (u_1, u_2)^T \in R^2$ is the vector of joint torques; and

$$B(x) = [I_{2 \times 2} \mid O_{2 \times 2n}]^T \quad (2.3)$$

where I , and O denote identity and null matrices of indicated dimensions. A complete derivation of equations of motion for the arm is given in [1] and readers may refer to it for

the details. However, in this study unlike [1], the strain energy due to deformation caused by gravitational force has been included in the potential energy. This is useful in computing the static deflection due to gravity in equilibrium condition.

Chapter 3

Decoupling Control

3.1 Introduction

The control system design to be presented here is based on nonlinear inversion and linear stabilization. The derivation of the controller presented here is done in two steps. This is motivated by the fact that nonlinearity in the dynamics of an elastic robotic system is essentially due to the rigid modes (joint angle variables) and once the time derivatives of rigid modes vanish, only elastic mode oscillation due to structural flexibility persists. The elastic dynamics has linear behavior, and is governed by linear differential equations.

In this chapter, first we obtain a nonlinear control law u_n based on the inversion of input (control torques) - output (joint angles) map. The use of feedback control law u_n decoupled the joint angle (rigid modes) motion from the elastic motion and gives linear dynamics for the joint angle trajectory tracking error.

The control law u_n also includes integral feedback of joint angle tracking error for robustness. The asymptotic motion of the closed-loop system using control u_n is nearly linear which includes small joint angles perturbation and bounded small oscillation of elastic modes. Ex-

exploiting the asymptotically linearized behavior of the closed-loop system with control u_n , a stabilizing control law u_s is designed for regulation to the terminal state. The motion of the system evolves in two phases.

In the first phase, the nonlinear control u_n acts and the arm follows any given smooth joint angle trajectory. In the second phase, once the joint angle enters a specified neighborhood of the terminal joint angle, the stabilizer is switched on and the total control signal ($u_n + u_s$) accomplishes final capture of the terminal joint angle and damping of elastic oscillation. The dual mode operation of the controller is useful in real-time control, since this gives the required time for the computation of stabilizer gain matrix. Therefore, a control logic has been introduced in the control system design which causes the closing of the stabilizer-loop only when the joint angle trajectory enters a specified vicinity of the terminal joint angle which must be the region of attraction of the terminal state. A compromise in the degree of joint angle trajectory tracking ability and stabilization must be made. Apparently, one would like to have the signal u_s of small value so that joint angle tracking is not much disturbed.

3.2 Problem Formulation

Using the expressions for K and V in (2.2) gives,

$$D(z)\ddot{z} + \dot{D}(z)\dot{z} - \frac{\partial K}{\partial z} + \frac{\partial V}{\partial z} = B_1 u \quad (3.1)$$

where D is the positive definite symmetric inertia matrix, and $K = \frac{1}{2} (\dot{z}^T D(z) \dot{z})$. Defining $x = (z^T, \dot{z}^T)^T$, (3.1) can be written as

$$\dot{x} = A(x) + B(x)u, \quad x \in R^{2k}, \quad k = (2 + 2n) \quad (3.2)$$

where A and B are appropriate matrices obtained from (3.1) and $B(x) = [O_{2 \times k} \quad | \quad B_1^T]^T$.

We point out that, for simplicity, the arguments of various functions are often omitted. Let $\theta_c(t) \in R^2$ denotes a reference joint angle trajectory, where it is assumed that $\theta_c(t)$ is obtained from the coordinates of the end effector using a nonlinear transformation. We associate with (3.2) the controlled output vector

$$y = \theta = cx = c_0z \quad (3.3)$$

We are interested in deriving a control law such that in the closed loop the joint angle vector $\theta(t)$ follows the command trajectory $\theta_c(t)$ and elastic oscillations are stabilized.

3.3 Joint Angle Control By System Inversion

In this section, a control law is derived for the trajectory control of joint angles based on the inversion of input (joint torques) - output (joint angles) map of the system (3.2) and (3.3). Readers may refer to [14, 15] in which inversion algorithms are given for obtaining inverse systems for nonlinear systems. Although, the inversion algorithm is applicable when actuator dynamics are present in the system, these actuator transfer functions are neglected in this study.

Using the inversion algorithm one obtains a sequence of systems by differentiation of the outputs and nonlinear transformations. By differentiating the output gives system 1 and system 2 of the form (Nonlinear transformations are not required here)

$$\begin{aligned} \text{System1 : } \dot{x} &= a(x) + B(x)u \\ \xi_1 &= \dot{\theta} = c_1(x) \end{aligned} \quad (3.4)$$

$$\begin{aligned} \text{System2 : } \dot{x} &= a(x) + B(x)u \\ \xi_2 &= \ddot{\theta} = c_2(x) + D_2(x)u \end{aligned} \quad (3.5)$$

where

$$\begin{aligned} c_2(x) &= c_0 D^{-1}(z) \left[-\dot{D}(z)\dot{z} + \frac{\partial K}{\partial z} - \frac{\partial V}{\partial z} \right] \\ D_2(x) &= c_0 D^{-1}(z) B_1 \end{aligned} \quad (3.6)$$

Since the inertia matrix $D(z)$ is a positive definite symmetric matrix, $D_2(x)$ is invertible for $x \in R^{2k}$. The inversion algorithm terminates here, and the tracking order of the system (3.2) and (3.3) is 2. System 2 is invertible and one chooses a control law of the form $u = u_n$ given by

$$u_n = D_2^{-1}(x) \left[-c_2(x) - G_2 \dot{\tilde{\theta}} - G_1 \tilde{\theta} - G_0 w + \ddot{\theta}_c \right] \quad (3.7)$$

where $G_2 = \text{diag}(g_{2i})$; $G_1 = \text{diag}(g_{1i})$; $G_0 = \text{diag}(g_{0i})$, $i=1,2$; tracking error $\tilde{\theta} = \theta - \theta_c$ and w is the output of a servocompensator

$$\dot{w} = \tilde{\theta} \quad (3.8)$$

In the control law u_n , the function w has been included for robustness in the system.

Substituting (3.7) in (3.5) gives linear dynamics for the tracking error governed by

$$\ddot{\tilde{\theta}} + G_2 \dot{\tilde{\theta}} + G_1 \tilde{\theta} + G_0 w = 0 \quad (3.9)$$

Differentiating (12) and using (3.8) gives

$$\ddot{\tilde{\theta}} + G_2\ddot{\tilde{\theta}} + G_1\dot{\tilde{\theta}} + G_0\tilde{\theta} = 0 \quad (3.10)$$

In the closed-loop system (3.2), (3.7) and (3.8), independent control of joint angles is accomplished by a proper choice of matrices G_i , $i=0,1,2$, and desirable stable responses for the joint angles are obtained.

Control law (3.7) requires second derivative of the command input θ_c since system (3.2) and (3.3) has tracking order 2. It is convenient to introduce a third order command generator of the form

$$\ddot{\theta}_c + P_2\dot{\theta}_c + P_1\theta_c + P_0\theta_c = P_0\theta^* \quad (3.11)$$

where θ^* is the desired terminal joint angle, and matrices P_i , $i=0,1,2$ are properly chosen to obtain desirable reference trajectories.

Using the control law (3.7), one can reproduce any smooth joint angle trajectory θ_c provided that

$$\tilde{\theta}(0) = \dot{\tilde{\theta}}(0) = \ddot{\tilde{\theta}}(0) = 0 \quad (3.12)$$

However, as the joint angles follow the reference trajectories, elastic modes are excited and it becomes necessary to design a stabilizer to damp the elastic oscillation.

3.4 Linear Stabilizer

In the closed-loop system (3.2), (3.7) and (3.8), $\theta(t) \rightarrow \theta^*$, the given terminal joint angle and $\dot{\theta}(t), \ddot{\theta}(t) \rightarrow 0$ as $t \rightarrow \infty$. Since elastic deformation is assumed to be small, and

the nonlinearity in (3.2) is essentially due to the rigid modes, interestingly the closed-loop dynamics of the system (3.2), (3.7) and (3.8) is nearly linear as $t \rightarrow \infty$ and the design of stabilizer using linear control theory is appropriate.

For a given reference trajectory $\theta_c(t)$ terminating at θ^* , one has $\dot{\theta}_c(\infty) = \ddot{\theta}_c(\infty) = 0$. The equilibrium state vector x^* is obtained by solving

$$a(x^*) + B(x^*)u(x^*) = 0 \quad (3.13)$$

Let z^* be the equilibrium value of z . In view of (3.1) and noting that $\dot{z}^* = 0$, and $\frac{\partial K}{\partial z} = 0$ at the equilibrium point, one must have

$$\frac{\partial V}{\partial z}(z^*) = (u^T(z^*), O_{2 \times 2n})^T \quad (3.14)$$

The first two equations in (3.14) are satisfied by the control $u(z^*)$ and remaining $2n$ equations in (3.14) are easily solved to obtain the equilibrium value $q^* = (q_{11}^*, \dots, q_{1n}^*, q_{21}^*, \dots, q_{2n}^*)^T$.

To this end, we linearize the closed-loop system (3.2), (3.7) and (3.8). Since $\ddot{\theta}$ -response is linear, we linearize the q -response. Let

$$D(z) = \begin{bmatrix} D_{11}(z) & D_{12}(z) \\ D_{21}(z) & D_{22}(z) \end{bmatrix} \quad (3.15)$$

where D_{11} is a 2×2 matrix. Then using (3.1) and neglecting the second order terms in (\dot{z}_i, \dot{z}_j) in (3.1), gives

$$D_{21}(z)(\ddot{\theta}) + D_{22}(z)(\ddot{q}) + \frac{\partial V}{\partial q} = 0 \quad (3.16)$$

Linearizing (3.16) gives

$$D_{21}(z^*)\Delta\ddot{\theta} + D_{22}(z^*)\Delta\ddot{q} = -K_q\Delta q - V_{\theta q}(z^*)\Delta\theta \quad (3.17)$$

where $\Delta\theta = \theta - \theta^*$, $\Delta q = q - q^*$ and K_q is the stiffness matrix,

$$\begin{aligned} \frac{\partial^2 V(z)}{\partial z \partial q} &= \left[\frac{\partial^2 V(z)}{\partial \theta \partial q}, \frac{\partial^2 V(z)}{\partial q \partial q} \right] \\ &\triangleq [V_{\theta q}(z), K_q] \end{aligned} \quad (3.18)$$

Here, ($m_j =$ mass of link j)

$$\begin{aligned} K_q &= \text{diag}(K_{q1}, K_{q2}) \\ K_{qi} &= \text{diag}(K_{qi1}, \dots, K_{qin}), \\ K_{qij} &= EI_i \int_0^{L_i} \left(\frac{\partial \phi_{ij}(x)}{\partial x} \right)^2 dx \end{aligned} \quad (3.19)$$

For the design of stabilizer, it will be assumed that $\theta_c(t)$ has attained the terminal value, that is, $\theta_c = \theta^*$, $\dot{\theta}_c = \ddot{\theta}_c = 0$, and thus $\ddot{\theta}(t) = \Delta\ddot{\theta}(t)$. We are interested in designing a stabilizing control of the form

$$u_s = D_2^{-1}(x)v \quad (3.20)$$

where v is determined later. Then the control law is

$$u = u_n + u_s \quad (3.21)$$

Using the control law (3.7), (3.8),(3.20) and (3.21) in (3.5), substituting $\Delta\ddot{\theta}$ in (3.16)

from the resulting equation, solving for $\Delta\ddot{q}$ and collecting $\Delta\ddot{\theta}$ and $\Delta\ddot{q}$ equations, gives

$$\begin{bmatrix} \Delta\ddot{\theta} \\ \Delta\ddot{q} \end{bmatrix} = \begin{bmatrix} -G_2\Delta\dot{\theta} - G_1\Delta\theta - G_0w + v \\ D_{22}^{-1}(z^*)\{D_{21}(z^*)(G_2\Delta\dot{\theta} + G_1\Delta\theta + G_0w - v) - V_{\theta q}(z^*)\Delta\theta - K_q\Delta q\} \end{bmatrix} \quad (3.22)$$

Defining $\tilde{x} = (\Delta\theta^T, \Delta q^T, \Delta\dot{\theta}^T, \Delta\dot{q}^T, w^T)^T$, one can write (3.22) in the state variable form

$$\dot{\tilde{x}} = \tilde{A}(z^*)\tilde{x} + \tilde{B}(z^*)v, \tilde{x} \in R^{(2k+2)} \quad (3.23)$$

where

$$\tilde{A}(z^*) = \begin{bmatrix} O_{k \times k} & I_{k \times k} & O_{k \times 2} \\ (-G_1, O) & (-G_2, O) & -G_0 \\ D_{22}^{-1}(D_{21}G_1 - V_{\theta q}, -K_q) & D_{22}^{-1}(D_{21}G_2, O) & D_{22}^{-1}D_{21}G_0 \\ (I_{2 \times 2}, O) & O & O \end{bmatrix}$$

$$\tilde{B}(z^*) = \begin{bmatrix} O_{k \times 2} \\ I_{2 \times 2} \\ -D_{22}^{-1}(z^*)D_{21}(z^*) \\ O_{2 \times 2} \end{bmatrix}$$

where O's denote null matrices of appropriate dimensions.

For the design of stabilizer we use pole assignment technique. It is interesting to note that six eigenvalues of the matrix \tilde{A} are specified by the choice of matrices G_i in (3.10), and the remaining eigenvalues of \tilde{A} lie on imaginary axis. One chooses a feedback control law of the form

$$v = -F\tilde{x} \quad (3.24)$$

such that the closed loop system matrix $A_{cl} = (\tilde{A} - \tilde{B}F)$ has a given set of stable eigenvalues.

To this end, a discussion on the choice of feedback matrix F is desirable. Noting that the signal v affects the tracking ability of the nonlinear control law u_n , it is desirable to choose small gain matrix F for stabilization. However, for obtaining good damping, the poles of \tilde{A} must be moved sufficiently far away to the left in the complex plane. Thus here the designer is faced with conflicting requirements. A good choice of pole assignment may require retaining the six poles of \tilde{A} associated with the rigid modes unchanged, and shifting the remaining imaginary poles of \tilde{A} to the left in the stable region of the complex plane keeping their imaginary parts unaltered. This way in general the stabilization is accomplished which

requires smaller control signal v resulting in only a little deterioration in joint angle tracking ability.

The synthesis of the complete closed-loop system (shown in Fig. 2) is done as follows. First the nonlinear controller u_n acts following any new command, and this causes the tracking of $\theta_c(t)$. The stabilizer is switched on when the trajectory enters a specified vicinity of the equilibrium point, which lies in its region of attraction. Let us define a neighbourhood N_s of the equilibrium point

$$N_s = \{x \in R^{2k} : |\Delta\theta_i| \leq \alpha, |\Delta\dot{\theta}_i| \leq \beta, i = 1, 2\} \quad (3.25)$$

Then the switching logic switches the stabilizer on at the instant t_s at which $x(t_s) \in N_s$ and keeps the stabilizer-loop closed for $t \geq t_s$. Since in the vicinity N_s , $\Delta\theta(t) \approx \tilde{\theta}(t)$, we may use $\tilde{\theta}(t)$ instead of $\Delta\theta(t)$ in the control signal v .

The closed-loop system is asymptotically stable. The integral feedback aids in nulling the steady-state error in the joint angles in the presence of uncertainty. Since the poles of the system are continuous functions of the robot arm parameters, they remain stable for small changes in these parameters. Although, it is extremely difficult to derive the stable range of parameter variations, simulation results will be presented to show that the closed-loop system has good robustness property.

3.5 Simulation Results

In this section, the results of digital simulation are presented. The nominal values of parameters are given in the appendix. For trajectory following, the matched initial conditions on $\theta(t)$

and $\theta_c(t)$ at $t=0$ are assumed. The initial conditions are $x(0) = 0$, $\theta_c(0) = \dot{\theta}_c(0) = \ddot{\theta}_c(0) = 0$, and $w(0) = 0$. The mode shapes $\phi_{i;j}$ are selected as clamped-free modes [1].

A command trajectory $\theta_c(t)$ was generated to control $\theta(0) = 0$ to $\theta^* = (90^\circ, 60^\circ)^T$. The matrices P_i of the command generator are taken as $P_i = p_i I_{2 \times 2}$, $i=0,1,2$ and are selected such that the poles associated with $\theta_{ci}(t)$, the i th component $\theta_c(t)$, are at $-2, -2 \pm j2$. The feedback matrices G_i are selected as $G_i = g_i I_{2 \times 2}$, $i=0,1,2$ and are set to yield poles associated with $\tilde{\theta}_i$ in (3.10), of values $-10, -10 \pm j10$, where $\tilde{\theta} = (\tilde{\theta}_1, \tilde{\theta}_2)^T$. These poles are chosen to obtain fast tracking error responses. It is assumed that the elastic deflection is adequately represented by the first two modes, i.e., $n=2$ in (2.1).

Let the set of eigenvalues, $\rho(\tilde{A}(z^*))$, of $\tilde{A}(z^*)$ be

$$\rho(\tilde{A}) = S_\theta \cup S_e \quad (3.26)$$

where S_θ , and S_e are sets of eigenvalues associated with the rigid modes and elastic modes respectively and

$$\begin{aligned} S_\theta &= \{-10, -10, -10 \pm j10, -10 \pm j10\} \\ S_e &= \{\pm j15, \pm j22.5, \pm j106, \pm j230\} \end{aligned} \quad (3.27)$$

The feedback matrix F of the stabilizer was chosen such that the set of eigenvalues $\rho(A_{cl})$ of the matrix A_{cl} is

$$\rho(A_{cl}) = S_\theta \cup S_{ef} \quad (3.28)$$

where $S_{ef} = \{-2 + r_e, r_e \in S_e\}$. Notice that in the closed-loop system the set of eigenvalues of S_θ is retained, and imaginary roots of S_e are simply moved to the left by 2 units in the complex plane. In the switching logic, the hypercube N , has dimension such that $\alpha = 5^\circ$,

$$\beta = 3^\circ/sec.$$

For compactness, the following notations will be used in the sequel:

$$\begin{aligned} \dot{\theta}_m = & (\max | \dot{\theta}_1 |, \max | \dot{\theta}_2 |) \text{ (deg/sec)}, u_m = (\max | u_1 |, \max | u_2 |), \text{ (Nm)}, (u_{e1}, u_{e2}) = \\ & (u_{e1}(L_1, t), u_{e2}(L_2, t)) \text{ (m)}, u_{em} = (\max | u_{e1}(L_1, t) |, \max | u_{e2}(L_2, t) |) \text{ (cm)} \text{ and } \tilde{\theta}_m = \\ & (\max | \tilde{\theta}_1 |, \max | \tilde{\theta}_2 |) \text{ (deg)}. \end{aligned}$$

3.5.1 A. Trajectory Control: Stabilizer Loop Open

To examine joint angle trajectory tracking ability of the nonlinear controller u_n , the closed-loop system (3.2), (3.7) and (3.8) was simulated and the stabilizer-loop was not closed. Selected responses are shown in Fig. 3. As predicted, the tracking error $\tilde{\theta}(t)$ was identically zero. The response time of θ was nearly 2.75 seconds. Manuever of the arm results in excitation of the elastic modes and figure shows persistant periodic oscillation of the elastic modes. Periodically varying control signal was required just to cancel the effect of elastic modes on the rigid modes. The maximum magnitudes were $\dot{\theta}_m = (74.8, 48.89)$ deg/sec, $u_{em} = (5.4, 2.49)$ cm, and $u_m = (224.6, 83.7)$ Nm.

3.5.2 B. Trajectory control and Stabilization : Nominal System

The complete closed-loop system (3.2), (3.7), (3.8) and (3.24) including the stabilizer was simulated to examine the joint-angle trajectory tracking and elastic mode stabilization capability of the controller. Selected responses are shown in Fig. 4. Notice that the switching logic closes the stabilizer-loop in 2.38 seconds when the trajectory enters the specified hypercube. As expected the θ -tracking error is identically zero before the stabilizer-loop closes.

A small transient in the θ -response is caused when the stabilizer-loop is closed. However, an insignificant θ -tracking error is observed. The desired position is attained in about 4.5 seconds. The maximum values were $\dot{\theta}_m = (74.8, 49.89)$ deg/sec, $u_{em} = (5.08, 2.49)$ cm, $u_m = (211.7, 83.7)$ Nm, and $\tilde{\theta}_m = (0.29, 0.104)$ deg.

3.5.3 C. Trajectory Control and stabilization : Lower payload

To show the effect of payload changes, simulation was done with $m_p=3$ kg. $J_p = .75$ which is 25% lower than the nominal payload. However the controller of case B designed using the nominal parameters was retained. Selected responses are shown in Fig. 5. The uncertainty in the payload caused only a small effect on system responses. Smaller elastic deflection was observed and smaller control torques were required compared to the nominal case B as expected. The maximum values were $\dot{\theta}_m = (74.9, 49.8)$ deg/sec, $u_{em} = (4.77, 1.9)$ cm, $u_m = (194, 67.2)$ Nm, and $\tilde{\theta}_m = (.11, .14)$ deg.

3.5.4 D. Trajectory Control and Stabilization: Higher payload

Controller was designed for the nominal payload as in case B, however the payload of the arm was increased by $\Delta m_p = .5$, $\Delta J_p = .125$ in simulation which amounts to 12.5% increase in payload. selected responses are shown in Fig. 6. Again accurate θ -trajectory tracking and elastic mode stabilization was observed. The elastic deflection and control torques were larger in this case compared to the nominal case B. The maximum values were $\dot{\theta}_m = (74.9, 49.7)$ deg/sec, $u_{em} = (5.37, 2.79)$ cm, $u_m = (225, 92)$ Nm, and $\tilde{\theta}_m = (.34, .107)$ deg. It was found that the controller was relatively sensitive to higher payload. This suggests that the

controller should be designed for maximum payload.

3.5.5 E. Trajectory Tracking and Stabilization: Effect of Pole Assignment

To show the importance of proper selection of poles of the closed-loop system matrix A_{cl} , a new feedback matrix F was designed by setting $\rho(A_{cl}) = S_\theta \cup S_{ef}$ where $S_{ef} = \{-2 \pm j20, -2 \pm j53, -2 \pm 233, -2 \pm j318\}$ and S_θ is given in (3.27). Compared to (30), we note that 8 closed-loop poles of A_{cl} in this case have larger imaginary parts compared to the poles of \tilde{A} or the matrix A_{cl} of case B. Selected responses are shown in Fig. 7. We observe undesirable high frequency oscillations in responses. This is caused due to modification in the natural oscillatory behavior of the closed-loop system (3.2), (3.7), and (3.8) of case A by the stabilizer. The maximum values were $\dot{\theta}_m = (74.8, 49.87)$ deg/sec, $u_{em} = (5.69, 2.5)$ cm, $u_m = (483, 269)$ Nm, and $\tilde{\theta}_m = (.57, .24)$ deg. We observed larger magnitude of elastic deflection and control torques compared to the nominal case B.

For this choice of poles of A_{cl} , simulation was also done in the presence of payload uncertainty and it was found that control system remains stable even for 75% lower and 25% higher payload changes (These results are not shown here). This suggests that proper selection of feedback gain matrix F is critical in the control system.

3.5.6 F. Trajectory Tracking and Stabilization: Slow Command

In order to reduce elastic deflections and control magnitude requirement, simulation was done using a slow command. For this purpose, poles of (3.11) were set at $-1, -1 \pm j1$.

Simulation was done under similar condition as in case B. Selected responses are shown in Fig. 8. Smooth responses were obtained. As expected smaller elastic deflection was observed and control magnitude was smaller. The maximum values were $\dot{\theta}_m = (37.4, 24.9)$ deg/sec, $u_{em} = (4.26, 1.84)$ cm, $u_m = (175, 63.5)$ Nm, and $\tilde{\theta}_m = (.14, .068)$ deg.

3.6 Conclusion

A dual mode control system design for control of a two-link elastic robotic system was presented. A nonlinear controller was designed for the independent control of joint angles using nonlinear inversion technique. Integral feedback was included in the nonlinear control law for robustness. Using pole assignment technique, a stabilizer was designed based on a linearized model about the terminal state. The system trajectory evolves in two phases. In the first phase, joint angles are controlled along prescribed paths. In the second phase, a switching logic turns on the stabilizer when the trajectory enters a specified neighborhood of the terminal state. Extensive simulation results were obtained which showed that in the closed-loop system accurate trajectory tracking and elastic mode stabilization can be accomplished.

Chapter 4

Effect of Coriolis and Centrifugal Forces

4.1 Introduction

The control system discussed so far includes an inverse joint angle trajectory following controller, a servocompensator, a linear stabilizer and a switching logic. A large amount of computation is required in the implementation of the exact inverse control law. A reasonable choice of simplification of the controller is to neglect the Coriolis and centrifugal forces from the joint angle controller. These forces contain terms of second order in the velocity of the generalized coordinates. In this study simplified control law by neglecting Coriolis and Centrifugal forces is synthesized. It is seen that for the slow motion of the arm, these forces are small, however, during rapid maneuver they are not negligible.

4.2 Problem Formulation

The equation of motion is,

$$D(z)\ddot{z} + \dot{D}(z)\dot{z} - \frac{\partial K}{\partial z} + \frac{\partial V}{\partial z} = B_1 u \quad (4.1)$$

where D is the positive definite symmetric inertia matrix, $B_1 = [I_{2 \times 2} O]^2$ and $K = \frac{1}{2} (\dot{z}^T D(z) \dot{z})$. The system (4.1) can be simplified by neglecting Coriolis and Cetrifugal terms.

The simplified equation is

$$D(z)\ddot{z} + \frac{\partial V}{\partial z} = B_1 u \quad (4.2)$$

Defining $x = (z^T, \dot{z}^T)^T$, (4.2) can be written as

$$\dot{x} = A(x) + B(x)u, \quad x \in R^{2k}, \quad k = (2 + 2n) \quad (4.3)$$

where A and B are appropriate matrices obtained from (4.2) and $B(x) = [O_{2 \times k} \quad (D^{-1} B_1)^T]^T$. We point out that, for simplicity, the arguments of various functions are often omitted. Let $\theta_c(t) \in R^2$ denotes a reference joint angle trajectory, where it is assumed that $\theta_c(t)$ is obtained from the coordinates of the end effector using a nonlinear transformation.

We associate with (4.3) the controlled output vector

$$y = \theta = cx = c_0 z \quad (4.4)$$

We are interested in deriving a control law such that in the closed loop the joint angle vector $\theta(t)$ follows the command trajectory $\theta_c(t)$ and elastic oscillations are stabilized.

4.3 Joint Angle Control

In this section, a control law is derived for the trajectory control of joint angles based on the inversion of input (joint torques) - output (joint angles) map of the system (4.2) and (4.3).

Using the inversion algorithm one obtains a sequence of systems by differentiation of the outputs and nonlinear transformations. By differentiating the output gives system 1 and system 2 of the form (Nonlinear transformations are not required here)

$$\begin{aligned} \text{System1: } \dot{x} &= a(x) + B(x)u \\ \xi_1 &= \dot{\theta} = c_1(x) \end{aligned} \quad (4.5)$$

$$\begin{aligned} \text{System2: } \dot{x} &= a(x) + B(x)u \\ \xi_2 &= \ddot{\theta} = c_2(x) + D_2(x)u \end{aligned} \quad (4.6)$$

where

$$\begin{aligned} c_2(x) &= c_0 D^{-1}(z) \left[-\frac{\partial V}{\partial z} \right] \\ D_2(x) &= c_0 D^{-1}(z) B_1 \end{aligned} \quad (4.7)$$

Since the inertia matrix $D(z)$ is a positive definite symmetric matrix, $D_2(x)$ is invertible for $x \in R^{2k}$. The inversion algorithm terminates here, and the tracking order of the system (4.2) and (4.3) is 2. System 2 is invertible and one chooses a control law of the form $u = u_n$ given by

$$u_n = D_2^{-1}(x) \left[-c_2(x) - G_2 \dot{\tilde{\theta}} - G_1 \tilde{\theta} - G_0 w + \ddot{\theta}_c \right] \quad (4.8)$$

where $G_2 = \text{diag}(g_{2i})$; $G_1 = \text{diag}(g_{1i})$; $G_0 = \text{diag}(g_{0i})$, $i=1,2$; tracking error $\tilde{\theta} = \theta - \theta_c$ and w is the output of a servocompensator

$$\dot{w} = \tilde{\theta} \quad (4.9)$$

In the control law u_n , the function w has been included for robustness in the system.

Substituting (4.8) in (4.5) gives linear dynamics for the tracking error governed by

$$\ddot{\tilde{\theta}} + G_2\dot{\tilde{\theta}} + G_1\tilde{\theta} + G_0w = 0 \quad (4.10)$$

Differentiating (4.10) and using (4.9) gives

$$\ddot{\tilde{\theta}} + G_2\ddot{\tilde{\theta}} + G_1\dot{\tilde{\theta}} + G_0\tilde{\theta} = 0 \quad (4.11)$$

In the closed-loop system (4.3), (4.8) and (4.9), independent control of joint angles is accomplished by a proper choice of matrices G_i , $i=0,1,2$, and desirable stable responses for the joint angles are obtained.

Control law (4.8) requires second derivative of the command input θ_c since system (4.2) and (4.3) has tracking order 2. It is convenient to introduce a third order command generator of the form

$$\ddot{\theta}_c + P_2\dot{\theta}_c + P_1\theta_c + P_0\theta_c = P_0\theta^* \quad (4.12)$$

where θ^* is the desired terminal joint angle, and matrices P_i , $i=0,1,2$ are properly chosen to obtain desirable reference trajectories.

4.4 Linear Stabilizer

In the closed-loop system (4.2), (4.8) and (4.9), $\theta(t) \rightarrow \theta^*$, the given terminal joint angle and $\dot{\theta}(t), \ddot{\theta}(t) \rightarrow 0$ as $t \rightarrow \infty$. Since elastic deformation is assumed to be small, and the nonlinearity in (4.2) is essentially due to the rigid modes, interestingly the closed-loop dynamics of the system (4.2), (4.8) and (4.9) is nearly linear as $t \rightarrow \infty$ and the design of stabilizer using linear control theory is appropriate.

Defining $\tilde{x} = (\Delta\theta^T, \Delta q^T, \Delta\dot{\theta}^T, \Delta\dot{q}^T, w^T)^T$, one can write the stabilizer equation in the state variable form

$$\dot{\tilde{x}} = \tilde{A}(z^*)\tilde{x} + \tilde{B}(z^*)v, \tilde{x} \in R^{(2k+2)} \quad (4.13)$$

where

$$\tilde{A}(z^*) = \begin{bmatrix} O_{k \times k} & I_{k \times k} & O_{k \times 2} \\ (-G_1, O) & (-G_2, O) & -G_0 \\ D_{22}^{-1}(D_{21}G_1 - V_{\theta q}, -K_q) & D_{22}^{-1}(D_{21}G_2, O) & D_{22}^{-1}D_{21}G_0 \\ (I_{2 \times 2}, O) & O & O \end{bmatrix}$$

$$\tilde{B}(z^*) = \begin{bmatrix} O_{k \times 2} \\ I_{2 \times 2} \\ -D_{22}^{-1}(z^*)D_{21}(z^*) \\ O_{2 \times 2} \end{bmatrix}$$

where O's denote null matrices of appropriate dimensions.

For the design of stabilizer we use pole assignment technique. It is interesting to note that six eigenvalues of the matrix \tilde{A} are specified by the choice of matrices G_i in (4.11), and the remaining eigenvalues of \tilde{A} lie on imaginary axis. One chooses a feedback control law of the form

$$v = -F\tilde{x} \quad (4.14)$$

such that the closed loop system matrix $A_{cl} = (\tilde{A} - \tilde{B}F)$ has a given set of stable eigenvalues.

4.5 Simulation Results

In this section, the results of digital simulation are presented. The nominal values of parameters are given in the appendix. For trajectory following, the matched initial conditions on $\theta(t)$ and $\theta_c(t)$ at $t=0$ are assumed. The initial conditions are $x(0) = 0$, $\theta_c(0) = \dot{\theta}_c(0) = \ddot{\theta}_c(0) = 0$,

and $w(0) = 0$. The mode shapes ϕ_{ij} are selected as clamped-free modes [1].

A command trajectory $\theta_c(t)$ was generated to control $\theta(0) = 0$ to $\theta^* = (90^\circ, 60^\circ)^T$. The matrices P_i of the command generator are taken as $P_i = p_i I_{2 \times 2}$, $i=0,1,2$ and are selected such that the poles associated with $\theta_{ci}(t)$, the i th component $\theta_c(t)$, are at $-2, -2 \pm j2$. The feedback matrices G_i are selected as $G_i = g_i I_{2 \times 2}$, $i=0,1,2$ and are set to yield poles associated with $\tilde{\theta}_i$ in (3.8), of values $-10, -10 \pm j10$, where $\tilde{\theta} = (\tilde{\theta}_1, \tilde{\theta}_2)^T$. These poles are chosen to obtain fast tracking error responses.

For compactness, the following notations will be used in the sequel:

$\dot{\theta}_m = (\max | \dot{\theta}_1 |, \max | \dot{\theta}_2 |)$ (deg/sec), $u_m = (\max | u_1 |, \max | u_2 |)$, (Nm), $(u_{e1}, u_{e2}) = (u_{e1}(L_1, t), u_{e2}(L_2, t))$ (m), $u_{em} = (\max | u_{e1}(L_1, t) |, \max | u_{e2}(L_2, t) |)$ (cm) and $\tilde{\theta}_m = (\max | \tilde{\theta}_1 |, \max | \tilde{\theta}_2 |)$ (deg).

4.5.1 A. Trajectory control and Stabilization : Nominal System

The complete closed-loop system (4.3), (4.8), (4.9) and (4.14) including the stabilizer was simulated to examine the differences between the simplified controller and the controller designed without simplification in [8]. Selected responses are shown in Fig. 9. There is not much difference in the θ tracking ability of the two controllers. Maximum values which are different are shown here for the two controllers. First for the complete controller of [8] $\dot{\theta}_m = (74.9, 49.8)$ deg/sec, $u_{em} = (5.08, 2.5)$ cm, $u_m = (211, 83.7)$ Nm and $\tilde{\theta}_m = (.294, .104)$ deg. For the simplified controller $\dot{\theta}_m = (75.7, 50.1)$ deg/sec, $u_{em} = (5.83, 2.676)$ cm, $u_m = (244, 85.7)$ Nm and $\tilde{\theta}_m = (.398, .149)$ deg. We observed larger magnitude of elastic deflection and

control torques compared to the controller of [8].

4.5.2 B. Trajectory Control and Stabilization: Higher payload

Controller was designed for the nominal payload as in case A, however the payload of the arm was increased by $\Delta m_p = .5$, $\Delta J_p = .125$ in simulation which amounts to 12.5% increase in payload. Selected responses are shown in Fig. 10. There is not much difference in the θ tracking ability of the two controllers. Maximum values which are different are shown here for the two controllers. First for the complete controller $\dot{\theta}_m = (74.9, 49.7)$ deg/sec, $u_{em} = (5.37, 2.79)$ cm, $u_m = (225, 92.1)$ Nm and $\tilde{\theta}_m = (.34, .11)$ deg. For the simplified controller $\dot{\theta}_m = (76, 49.9)$ deg/sec, $u_{em} = (6.12, 3.02)$ cm, $u_m = (259, 95.1)$ Nm and $\tilde{\theta}_m = (.45, .15)$ deg. As in case A larger control torques and elastic mode deflections were observed.

4.5.3 C. Trajectory Control and stabilization : Fast System

In order to show the effect on deflections and control magnitude requirement for fast movement, simulation was done using a fast command. For this purpose, poles of (4.10) were set at $-4, -4 \pm j4$. Simulation was done under similar condition as in case A. Selected responses are shown in Fig. 11. There is not much difference in the θ tracking ability of the two controllers. Maximum values which are different are shown here for the two controllers. First for the complete controller $\dot{\theta}_m = (149, 99.7)$ deg/sec, $u_{em} = (15, 10.6)$ cm, $u_m = (768, 332)$ Nm and $\tilde{\theta}_m = (1.485, .966)$ deg. For the simplified controller $\dot{\theta}_m = (189, 193)$ deg/sec, $u_{em} = (31.8, 17.7)$ cm, $u_m = (1338, 468)$ Nm and $\tilde{\theta}_m = (4.925, 4.926)$ deg. As in case A larger control torques and elastic mode deflection were observed.

4.6 Conclusions

A dual mode control system design for control of a two-link elastic robotic system was presented. A nonlinear controller was designed for the independent control of joint angles using nonlinear inversion technique. Integral feedback was included in the nonlinear control law for robustness. Using pole assignment technique, a stabilizer was designed based on a linearized model about the terminal state. Extensive simulation has been done. It is concluded from these results that accurate trajectory tracking and elastic stabilization are accomplished even when Coriolis and Centrifugal forces are neglected for reasonable fast motion. Furthermore, the joint angle tracking performance is relatively insensitive even for faster motion. However, the elastic deflection response and control torques are sensitive to neglected Coriolis and Centrifugal forces in the simplified controller.

Chapter 5

Adaptive control

5.1 Introduction

The control system design to be presented here is based on nonlinear adaptive control and linear stabilization. The derivation of the controller presented here treats the large joint-angle (nonlinear) maneuver problem separately from the small terminal (linear) maneuver. This is motivated by the fact that nonlinearity in the dynamics of an elastic robotic system is essentially due to the rigid modes (joint angle variables) and once the time derivatives of rigid modes vanish, only elastic mode oscillation due to structural flexibility persists. The elastic dynamics has linear behavior, and is governed by linear differential equations.

In this thesis first we derive a nonlinear adaptive control law u_a for joint angle trajectory tracking of reference trajectories. Interestingly, this design does not require any information on the system dynamics of the arm and the bounds on the uncertainty of the system used in sliding mode control [23]. The controller includes a dynamic system in the feedback path. This adaptive controller is simple to implement since it does not require the computation of complicated functions unlike the inverse control technique. Only joint angles and

their derivatives are required for feedback. Although, the adaptive controller accomplishes joint angle trajectory tracking it excites the elastic modes. Exploiting the asymptotically linearized behavior of the closed-loop system, a stabilizing control law u_s is designed for regulation to the terminal state. The motion of the system evolves in two phases. In the first phase, the nonlinear control u_a acts and the arm follows any given smooth joint angle trajectory. In the second phase, once the joint angle trajectory enters a specified neighborhood of the terminal joint angle, the stabilizer is switched on and the control signal u_s accomplishes final capture of the terminal state and damping of elastic oscillation. The dual mode operation of the controller is useful in real-time control, since this gives the required time for the computation of stabilizer gain matrix. It may be pointed out that the adaptive controller presented here differs from that of [13] in which a different robotic arm having one elastic link and two rigid links has been considered. Moreover, unlike [13], no additional actuators acting on the end effector are used for stabilization in this control scheme. For the implementation of a stabilizer in the final phase of maneuver, elastic modes are required for feedback. The estimate of these variables can be obtained by a Luenberger observer and using sensors such as strain gauges, accelerometers, and optical devices, etc.

5.2 Problem Formulation

Consider the system,

$$D(z)\ddot{z} + \dot{D}(z)\dot{z} - \frac{\partial K}{\partial z} + \frac{\partial V}{\partial z} = B_1 u \quad (5.1)$$

We assume that $z \in \Omega$, a open, bounded set in $R^{2(n+1)}$. We point out that, for simplicity, the arguments of various functions are often omitted. Let $\theta_c(t) \in R^2$ denotes a reference joint angle trajectory. Consider a reference model of the form

$$\ddot{\theta}_c(t) = -C\dot{\theta}_c(t) - K(\theta_c(t) - r) \quad (5.2)$$

where $K = \text{diag}(\omega_{ni}^2)$, $C = 2\text{diag}(\zeta_i\omega_{ni})$, $i = 1, 2$, $\zeta_i > 0$, $\omega_{ni} > 0$, and $r \in R^2$ is an external input.

We are interested in deriving a control law such that in the closed loop the joint angle vector $\theta(t)$ follows the command trajectory $\theta_c(t)$ and elastic oscillations are stabilized.

5.3 Adaptive Control of Joint Angles

In this section, a nonlinear adaptive joint angle controller based on the results of [27, 15] is designed. For this purpose, we consider the differential equations for the joint angles given by

$$\begin{aligned} \ddot{\theta} &= M_1(z) \left[-\dot{D}\dot{z} + \frac{\partial K}{\partial z} - \frac{\partial V}{\partial z} \right] + M_{11}(z)u \\ &\triangleq f_0(z, \dot{z}) + M_{11}(z)u \end{aligned} \quad (5.3)$$

where $D^{-1}(z) = M = [M_1^T, M_2^T]^T$, $M_1 = [M_{11}, M_{12}]$, M_{11} is a 2×2 positive definite symmetric matrix, and $f_0(z, \dot{z}) = M_1 \left[-\dot{D}\dot{z} + \frac{\partial K}{\partial z} - \frac{\partial V}{\partial z} \right]$. For the derivation of the controller, M_{11} and f_0 are treated as unknown functions. Define $e = (\tilde{\theta}^T, \dot{\tilde{\theta}}^T)^T$, where $\tilde{\theta} = \theta - \theta_c$. Then using (5.1) and (5.3) gives

$$\begin{aligned} \dot{e} &= \begin{bmatrix} 0 & I \\ -K & -C \end{bmatrix} e + \begin{bmatrix} 0 \\ I \end{bmatrix} [f_1 + M_{11}u] \\ &\triangleq Ae + B[f_1 + M_{11}u] \end{aligned} \quad (5.4)$$

where A, and B are defined in (5.4) and

$$f_1(z, \dot{z}, r) = f_0(z, \dot{z}) + C\dot{\theta} + K(\theta - r) \quad (5.5)$$

We note that A is a Hurwitz matrix.

Now a bound on the f_1 is obtained which is useful in the derivation of the control law.

In view of (5.3), f_0 can be written as

$$f_0(z, \dot{z}) = L_2(z, \dot{z}) + L_1(\theta)q + L_0(z) \quad (5.6)$$

where elements of L_2 are sum of quadratic functions of the velocity of the generalized coordinates. Assuming that $q, \dot{q}, \theta_c, \dot{\theta}_c$ and r are bounded functions, in view of (5.5), it can easily shown that for some real numbers $b_i > 0$,

$$\begin{aligned} \| f_1(z, \dot{z}, r) \| &\leq \| f_0(z, \dot{z}) + c\dot{\theta} + K\theta - Kr \| \\ &\leq b_1 \| \tilde{\theta} \| + b_2 \| \dot{\tilde{\theta}} \| + b_3 \| \dot{\tilde{\theta}} \|^2 + b_4 + b_5 \| q \| + b_6 \| \dot{q} \| \| \dot{\theta} \| + b_7 \| \dot{q} \|^2 \\ &\triangleq \Pi_1(z, \dot{z}, b) \end{aligned} \quad (5.7)$$

where $b = (b_1, \dots, b_7)$. To this end, let us evaluate

$$\begin{aligned} u^T [f_1 + M_{11}u] &\geq \beta_0 \| u \|^2 - \| u \| \Pi_1(z, \dot{z}, b) \\ &= \beta_0 \| u \| [\| u \| - \Pi(z, \dot{z}, \beta)] \end{aligned} \quad (5.8)$$

where

$$\begin{aligned}
\beta_0 &= \inf \{ \lambda_{\min}[M_{11}(z), z \in \Omega] \} \\
\Pi(z, \dot{z}, \beta) &= \beta_1 \|\tilde{\theta}\| + \beta_2 \|\dot{\tilde{\theta}}\| + \beta_3 \|\dot{\tilde{\theta}}\|^2 + \beta_4 + \beta_5 \|q\| + \beta_6 \|\dot{q}\| \|\dot{\theta}\| + \beta_7 \|\dot{q}\|^2 \quad (5.9) \\
\beta &= (\beta_1, \dots, \beta_7)^T \\
\beta_i &= b_i/\beta_0, i = 1, \dots, 7
\end{aligned}$$

Here $\lambda_{\min}[M_{11}]$ denotes the minimum eigenvalue of M .

Since A is a stable matrix, for a given symmetric positive definite matrix Q (denoted as $Q > 0$), there exist a unique $P > 0 \ni$

$$PA + A^T P = -Q \quad (5.10)$$

Now we chose a control law of the form

$$\begin{aligned}
\dot{\hat{\beta}}(t) &= N[\|\tilde{\theta}\|, \|\dot{\tilde{\theta}}\|, \|\dot{\tilde{\theta}}\|^2, 1, \|q\|, \|\dot{q}\| \|\dot{\theta}\|, \|\dot{q}\|^2]^T \cdot \|\alpha(e)\| \\
\dot{\epsilon}(t) &= -n_8 \epsilon(t), \epsilon(0) > 0. \\
u(t) &= -\Pi(z, \dot{z}, \hat{\beta}) \nu(e, \hat{\beta}, \epsilon)
\end{aligned} \quad (5.11)$$

where N is a diagonal matrix $N = \text{diag}(n_{ii}), i=1, \dots, 7; n_{ii} > 0, \hat{\beta} \in (0, \infty)^7$,

$$\alpha(e) = 2B^T P e \quad (5.12)$$

and the function ν is given by

$$\nu(e, \hat{\beta}, \epsilon) = \text{sat}[2\Pi(z, \dot{z}, \hat{\beta})B^T P e/\epsilon] \quad (5.13)$$

where for any $\eta \in R^2$,

$$\text{sat}\{\eta\} = \begin{cases} \eta & \|\eta\| \leq 1 \\ \eta/\|\eta\| & \|\eta\| > 1 \end{cases}$$

Theorem : Consider the closed-loop system (5.1), and (5.11). Suppose that the trajectory (q, \dot{q}) remains bounded. Then the equilibrium state $(e = 0, \beta, \epsilon = 0)$ of the system (5.4), (5.11) is stable and $\| e(t) \| \rightarrow 0$ as $t \rightarrow \infty$.

Proof: For a proof one chooses a Lyapunov function

$$W = e^T P e + \frac{\beta_0}{2} (\hat{\beta} - \beta)^T N^{-1} (\hat{\beta} - \beta) + \left(\frac{\beta_0}{n_8} \right) \epsilon \quad (5.14)$$

and shows that along the trajectory of the closed-loop system

$$\dot{W}(t) \leq -e^T Q e \quad (5.15)$$

Assuming that q and \dot{q} are bounded, the arguments in the proof is a simple extension of those of [13], therefore the details are omitted.

Remark 1: Under the assumption of boundedness of q and \dot{q} , the control law can be simplified as follows. When q and \dot{q} are bounded, (5.7) gives for some real numbers $a_i > 0$

$$\| f_1(z, \dot{z}, r) \| \leq a_1 \| \tilde{\theta} \| + a_2 \| \dot{\tilde{\theta}} \| + a_3 \| \dot{\tilde{\theta}} \|^2 + a_4 \quad (5.16)$$

and there exist $\beta_i > 0, i = 1, \dots, 4$ such that

$$\Pi(\tilde{\theta}, \dot{\tilde{\theta}}, \beta) = \beta_1 \| \tilde{\theta} \| + \beta_2 \| \dot{\tilde{\theta}} \| + \beta_3 \| \dot{\tilde{\theta}} \|^2 + \beta_4 \quad (5.17)$$

Thus β_5, \dots, β_7 are set to zero in (5.9). Such a simplified control law has been used in [13]

for controlling a 3-link arm with only one flexible link.

The assumption of boundedness of the flexible modes is not unrealistic. Note that as $(\tilde{\theta}(t), \dot{\tilde{\theta}}(t))$ tends to zero as $t \rightarrow \infty$, the only motion remaining in the system is due to elastic oscillation caused by the excitation of the elastic modes during maneuver of the arm. Simulation results (to be presented later) confirm that once joint angles have stabilized, the elastic modes exhibit bounded, periodic oscillations.

5.4 Linear Stabilizer

In the closed-loop system (5.1) and (5.9), $\theta(t) \rightarrow \theta^*$, the given terminal joint angle and $\dot{\theta}(t), \ddot{\theta}(t) \rightarrow 0$ as $t \rightarrow \infty$. Since elastic deformation is assumed to be small, and the nonlinearity in (5.1) is essentially due to the rigid modes, interestingly the closed-loop dynamics of the system (5.1), and (5.9) is nearly linear as $t \rightarrow \infty$ and the design of stabilizer using linear control theory is appropriate.

For a given reference trajectory $\theta_c(t)$ terminating at θ^* , one has $\dot{\theta}_c(\infty) = \ddot{\theta}_c(\infty) = 0$. Let $z^* = (\theta^T = \theta^{*T}, q^T = q^{*T}, \dot{\theta}^T = 0, \dot{q}^T = 0)^T$ be the equilibrium state of the closed-loop system (5.1). The vector q^* is obtained by solving

$$\frac{\partial V(z^*)}{\partial z_i} = 0, i = 3, \dots, 2n + 1 \quad (5.18)$$

where z_i are the elements of z . Let

$$u^* = [\partial V(z^*) / \partial \theta] \quad (5.19)$$

be the torque required to keep the arm at the equilibrium state.

Linearizing (5.1) about the equilibrium state, gives

$$D(z^*)\Delta\ddot{z} + \frac{\partial^2 V(z^*)}{\partial z \partial z} \Delta z = B_1 \Delta u \quad (5.20)$$

where $\Delta z = z - z^*$, and $\Delta u = u - u^*$.

To this end, in order to obtain robustness in the control system we introduce, a servo-compensator of the form

$$\dot{z}_s(t) = \Delta\theta(t) \quad (5.21)$$

Defining the state vector $\Delta\dot{x} = [\Delta z^T, \Delta\dot{z}^T, z_s^T]^T \in R^{2k}$, $k = (n + 2)$, the system (5.20) and (5.21) can be written in state variable form

$$\begin{aligned} \Delta\dot{x} &= \begin{bmatrix} 0 & I & 0 \\ A_{22} & 0 & 0 \\ I & 0 & 0 \end{bmatrix} \Delta x + \begin{bmatrix} 0 \\ B_2 \\ 0 \end{bmatrix} \Delta u \\ &\triangleq A \Delta x + B \Delta u \end{aligned} \quad (5.22)$$

where 0, and I denote appropriate null and identity matrices, $A_{22} = -D^{-1}(z^*) \frac{\partial^2 V(z^*)}{\partial z \partial z}$, and B_2 consists of the first two columns of $D^{-1}(z^*)$.

For the design of the stabilizer, we use the pole placement technique, and obtain a linear feedback control law $\Delta u = -F \Delta x$ to obtain desirable pole locations of the closed-loop system matrix $A_{cl} = (A - BF)$. Then the control signal for stabilization is

$$u_s(t) = u^* - F\Delta x \quad (5.23)$$

The feedback matrix was chosen such that the poles of the A_{cl} have the same imaginary parts as those of A and the real parts were shifted to left of the imaginary axis to obtain stable poles..

For the synthesis of the control law in the final phase of the motion, one can set $\Delta\theta = \theta - \theta_c$ and $\Delta\dot{\theta} = \dot{\theta} - \dot{\theta}_c$ since $\theta_c = \theta^*$ and $\dot{\theta}_c \approx 0$. It turns out the resulting feedback law gives smoother responses.

The synthesis of the complete closed-loop system (shown in Fig. 12) is done as follows. First the nonlinear controller u_a acts following any new command, and this causes the tracking of $\theta_c(t)$. The stabilizer is switched on when the trajectory enters a specified vicinity of the equilibrium point, which lies in its region of attraction and the adaptive controller is switched off. Let us define a neighbourhood N_s of the equilibrium point

$$N_s = \{x \in R^{2k} : |\Delta\theta_i| \leq \alpha, |\Delta\dot{\theta}_i| \leq \beta, i = 1, 2\} \quad (5.24)$$

Then the switching logic switches the stabilizer on at the instant t_s at which $x(t_s) \in N_s$ and keeps the stabilizer-loop closed for $t \geq t_s$.

To this end, a discussion on the robustness of the control system is appropriate. It is interesting to note that if one uses the adaptive control law, no matter what payload is, the joint angle tracking error converges to zero for any large maneuver. However, the design of stabilizer requires the knowledge of the inertia matrix and the expression for the potential energy

at the equilibrium point. The closed-loop system with the linear stabilizer is asymptotically stable. The integral feedback aids in nulling the steady-state error in the joint angles in the presence of uncertainty. Since the poles of the system are continuous functions of the robot arm parameters, they remain stable for small changes in these parameters. Although, it is extremely difficult to derive the stable range of parameter variations, simulation results will be presented to show that the closed-loop system has good robustness property.

It should be pointed out that if one uses the adaptive controller given in Remark 1; the feedback of only joint angle tracking error and its derivative are required, and no information on the flexible modes are needed during the first phase of motion of the arm. Since the complete state feedback is required only in the final phase, a linear stabilizer will be adequate to estimate the state variables.

5.5 Simulation Results

In this section, the results of digital simulation of the closed-loop system (5.1), (5.2), (5.11) with the simplified function $\Pi(\tilde{\theta}, \dot{\tilde{\theta}}, \hat{\beta})$ are given in (5.17), and (5.23) are presented. The nominal values of parameters are given in the appendix. For trajectory following, the matched initial conditions on $\theta(t)$ and $\theta_c(t)$ at $t=0$ are assumed. The initial conditions are $z(0) = 0$, $\dot{z}(0) = 0$, $\theta_c(0) = \dot{\theta}_c(0)$ and $z_s(0) = 0$. The mode shapes ϕ_{ij} are selected as clamped-free modes [1].

A command trajectory $\theta_c(t)$ was generated to control $\theta(0) = 0$ to $\theta^* = (90^\circ, 60^\circ)^T$. For the purpose of simulation we set $\zeta_i = 0.707$, $\omega_{ni} = \frac{2}{\zeta_i}$, $i = 1, 2$ in the command generator.

The following constants are used in the simulation: $Q = I$, $\hat{\beta}(0) = [200., 200., 200., 200.]^T$, $\epsilon(0) = 0.1$, $N = \text{diag}(100., 100., 100., 100.)$, $n_8 = 0.2$. The values of the design parameters were obtained by observing the simulated responses and trial and error.

For compactness, the following notations will be used in the sequel:

$\dot{\theta}_m = (\max |\dot{\theta}_1|, \max |\dot{\theta}_2|)$ (deg/sec), $u_m = (\max |u_1|, \max |u_2|)$, (Nm), $(u_{e1}, u_{e2}) = (u_{e1}(L_1, t), u_{e2}(L_2, t))$ (m), $u_{em} = (\max |u_{e1}(L_1, t)|, \max |u_{e2}(L_2, t)|)$ (cm) and $\tilde{\theta}_m = (\max |\tilde{\theta}_1|, \max |\tilde{\theta}_2|)$ (deg).

5.5.1 A. Trajectory control and Stabilization : Nominal System

The complete closed-loop system (5.1), (5.11), (5.17) and (5.23) including the stabilizer was simulated to examine the joint-angle trajectory tracking and elastic mode stabilization capability of the controller. Selected responses are shown in Fig. 3. The stabilizer-loop is closed at $t = 3$ seconds. Joint angle tracking error is small before the stabilizer-loop closes, however a small transient in the θ -response is caused when the stabilizer-loop is closed. This is natural, since torquer can stabilize the vibrating link only by varying θ . The desired position is attained in about 18 seconds. The maximum values were $\dot{\theta}_m = (75.136, 95.67)$ deg/sec, $u_{em} = (4.09, 2.359)$ cm, $u_m = (470.1, 459.94)$ Nm, and $\tilde{\theta}_m = (5.6979, 5.0559)$ deg.

To examine whether the adaptive controller was necessary for controlling the arm, simulation was done without the adaptive controller and the linear stabilizer was switched on right from the instant $t = 0$. In the closed-loop system unbounded system responses were obtained. This shows the importance of the adaptive controller in accomplishing stable large

joint-angle maneuver.

5.5.2 B. Trajectory Control and stabilization : Lower payload

To show the effect of payload changes, simulation was done with $m_p=3.75$ kg and $J_p = .9375$ which is 6.25% lower than the nominal payload. Selected responses are shown in Fig. 4. However the controller of case A designed using the nominal parameters was retained. For this amount of uncertainty in the payload, responses some what close to case A were obtained. Larger torques were required to control the arm. Joint angle tracking error was larger in this case. This is due to the fact that the control parameters have been tuned to get good responses in case A. The maximum values were $\dot{\theta}_m = (75.38, 50.34)$ deg/sec, $u_{em} = (4.13, 2.24)$ cm, $u_m = (498., 466.)$ Nm, and $\tilde{\theta}_m = (10.8, 10.7)$ deg. It is found that the controller is sensitive to lower payload.

5.5.3 C. Trajectory Control and Stabilization: Higher payload

Controller was designed for the nominal payload as in case A, however the payload of the arm was increased by $\Delta m_p = 0.5$, $\Delta J_p = 0.125$ in simulation which amounts to 12.5% increase in payload. Selected responses are shown in Fig. 5. Again accurate θ -trajectory tracking and elastic mode stabilization was observed. The elastic deflection and control torques were larger in this case compared to the nominal case B. The maximum values were $\dot{\theta}_m = (74.7, 50.3)$ deg/sec, $u_{em} = (4.29, 2.66)$ cm, $u_m = (487, 465)$ Nm, and $\tilde{\theta}_m = (5.69, 5.05)$ deg. It was found that the controller was relatively less sensitive to higher payload than the lower payload.

5.6 Conclusion

A nonlinear adaptive control system was designed for joint angle control. The adaptive controller can be easily implemented since it does not require the computation of complicated functions unlike inverse control and it is a simple function of the tracking error. The stabilizer was designed based on the asymptotically linearized model of the closed loop system. Extensive simulation results were obtained which showed that in the closed-loop system accurate trajectory tracking and elastic mode stabilization can be accomplished.

For the implementation of the stabilizer the elastic modes are required for feedback. The missing states can be constructed by an observer using sensor data. It is pointed out that although, the joint angle control is accomplished by the nonlinear adaptive controller, the design of the stabilizer requires the knowledge of linearized model. It will be useful to design a linear adaptive stabilizer for the final capture of the terminal state. This will result in a complete adaptive control system. Some of the questions are presently being examined.

Chapter 6

Conclusion

A dual mode controller for the control of a two-link elastic robotic system was presented. The nonlinear controller was designed for the purpose of joint angle control and a linear stabilizer was used to dampen the elastic modes. The system evolves in two phases. In the first phase the nonlinear controller is acting and in the second phase the stabilizer is switched on. In the case of the adaptive controller the nonlinear controller is completely switched off and the stabilizer alone is used to obtain the final capture of the system. Extensive simulation has been done. The results indicate accurate trajectory tracking and elastic mode stabilization.

There are several open questions that remain to be answered in this area. Synthesis of controller using only measured variables needs attention. Of course elastic modes can be determined using strain gauges as in [12]. The choice of poles for robustness is extremely important. The delay in the actuators is not considered in the simulation.

Bibliography

1. O. Maizza-Neto, "Modal analysis and control of flexible manipulator arms," Ph.D Thesis, Department of Mechanical Engineering, M.I.T., Cambridge, 1973.
2. W. J. Book, O. Maizza-Neto, and D. E. Whitney, "Feedback control of two beam, two joint systems with distributed flexibility," *Journal of Dynamic Systems, Measurements and Control.*, vol 94, 4, pp. 424-431, Dec. 1975.
3. R. P. Judd and D. R. Falkenberg, " Control strategy for flexible robot mechanism," in *Proceedings of the 15th Southeastern Symposium on System Theory*, Mar. 1983.
4. W. J. Book and M. Majette, "Controller strategy for flexible distributed parameter mechanical arm via combined state space frequency domain techniques," *Journal of Dynamic Systems, Measurements and Control.*, vol 105, pp. 245-254, Dec. 1983.
5. P. B. Usora, R. Nadira, and S. S. Mahil, "Control of lightweight flexible manipulators: A feasibility Study," in *Proceedings of the 1984 American Control Conference.*, pp. 1209-1216, 1984.
6. N. G. Chalhoub, and A. G. Ulsoy, "Control of a flexible robot arm: experimental

- and theoretical results," *Journal of Dynamic Systems, Measurements and Control.*, pp. 299-309, Dec. 1987.
7. P. B. Usora, R. Nadira, S. S. Mahil, and R. K. Mehra, "Advanced control of flexible manipulators," *Final Report ECS-8260419, Scientific Systems Inc. Mass.*, Apr. 1983.
 8. A. Das and S. N. Singh, "Dual mode control of an elastic robotic arm: nonlinear inversion and stabilization by pole assignment," *American Control Conference*, Vol. 2, pp. 1598-1603, June 1989.
 9. S. N. Singh and A. A. Schy, "Elastic robot control: nonlinear inversion and linear stabilization," *IEEE Transactions on Aerospace and Electronic Systems*, vol 22, pp. 340-348, Sept. 1986.
 10. S. N. Singh and A. A. Schy, "Control of elastic robotic systems by nonlinear inversion and modal damping," *Journal of Dynamic Systems, Measurements and Control.*, vol. 108, pp. 180-189, Sept. 1986.
 11. R. H. Canon Jr., and E. Schmitz, "Initial experiments on the end-point control of a one link flexible experimental manipulator," *International Journal of Robotics Research.*, vol. 3, Fall. 1986.
 12. D. C. Nemir, A. J. Koivo, and R. L. Kashyap, "Pseudolinks and the self-tuning control of a nonrigid link mechanism," *IEEE Transactions on Systems, Man and Cybernetics*,

vol. 18, pp. 40-48, Jan/Feb 1988.

13. S. N. Singh, "Control and stabilization of a nonlinear uncertain elastic arm," *IEEE Transactions on Aerospace and Elastic Systems*, pp. 148-155, March 1988.
14. R. M. Hirshorn, "Output tracking in multivariable nonlinear systems," *IEEE Transactions on Automatic Control*. AC-26, pp. 595-598, 1981.
15. S. N. Singh, "A modified algorithm for invertibility in nonlinear systems," *IEEE Transactions on Automatic Control*, pp. 595-598, April 1981.
16. V. V. Korolov and Y. H. Chen, "Controller design robust to frequency variation in a one-link flexible robot arm", *Journal of Dynamic Systems, Measurement, and control*, Vol. 111/9, March 1989.
17. P. T. Kotnik, S. Yurkovich and U. Özgüner, "Acceleration feedback for control of a flexible manipulator arm," *Journal of Robotic Systems*, 5(3), 181-196 (1988).
18. B. Siciliano, Wayne J. Book 1988, "A Singular Perturbation approach to control of Lightweight Flexible Manipulators", *The International Journal of Robotics research*, vol.7, No.4, 1988, pp 79-88.
19. T. Yang, K. Sung, J. C. S. Yang, and P. Kudva, "An experimental adaptive control scheme for a flexible manipulator," *International Journal of robotics and Automation*, Vol 3, No 2, 1988, pp 79-85.

20. D. M. Rovner and G. F. Franklin, "Experiments in load-adaptive control of a very flexible one-link manipulator", *Automatica*, Vol. 24, No. 4, pp. 541-548, 1988.
21. S. Yurkovich, F. E. Pacheco, A. P. Tzes, "On-line frequency domain information for control of a flexible-link robot with varying payload", *IEEE International conference on Robotics and Automation*, 1989, Vol. 2, pp. 876-881.
22. A. J. Koivo and K. S. Lee, "Self-Tuning control of planar two-link manipulator with non-rigid arm", *IEEE International conference on Robotics and Automation*, 1989, Vol. 2, pp. 1030-1041.
23. P. J. Nathan, and S. N. Singh, "Variable Structure control of a robotic arm with flexible links", *IEEE International Conference on Robotics and Automation*, Scottsdale, Arizona, May 1989, pp 882-887.
24. H. Sira-Ramirez and M. W. Spong, "Variable Structure control of flexible joint manipulators", *International Journal of Robotics and Automation*, Vol 3, No. 2, 1988, pp. 57-64.
25. K. Khorasani, "Invariant manifolds and their application to robot manipulators with flexible joints", *IEEE International Conference on Robotics and Automation*, May 1989, Vol. 2, pp. 1194-1199.
26. K. Chen and L. Fu, "Nonlinear Adaptive Motion control for a manipulator with flexible joints", *IEEE International Conference on Robotics and Automation*, May 1989, Vol.

2, pp. 1201-1206.

27. M. Corless and G. Leitmann, "Adaptive control of systems containing uncertain functions and unknown functions with uncertain bounds.", *Journal of Optimization and theory Applications*, 41, Sept. 1983, pp. 158-168.
28. S. N. Singh, "Adaptive model following control of nonlinear robotic systems", *IEEE Transactions on Automatic Control*, 30, Nov. 1985, pp. 1099-1100.
29. A. Das, and S. N. Singh, "Inverse Control and Stabilization of Elastic Arm: Effect of Coriolis and Centrifugal Forces.", *ISMM International Symposium Computer Applications in Design, Simulation, and Analysis*, MIMI '89, pp. 262-265.

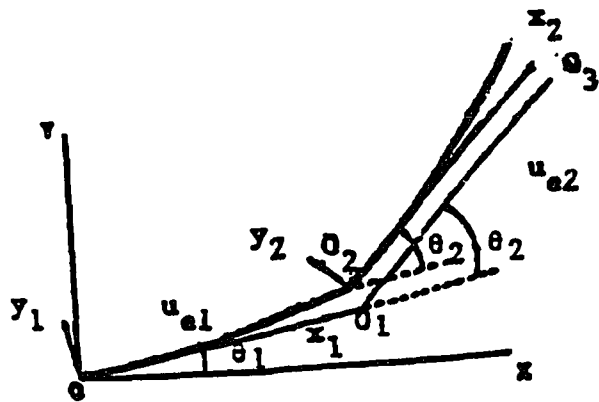


Figure 1

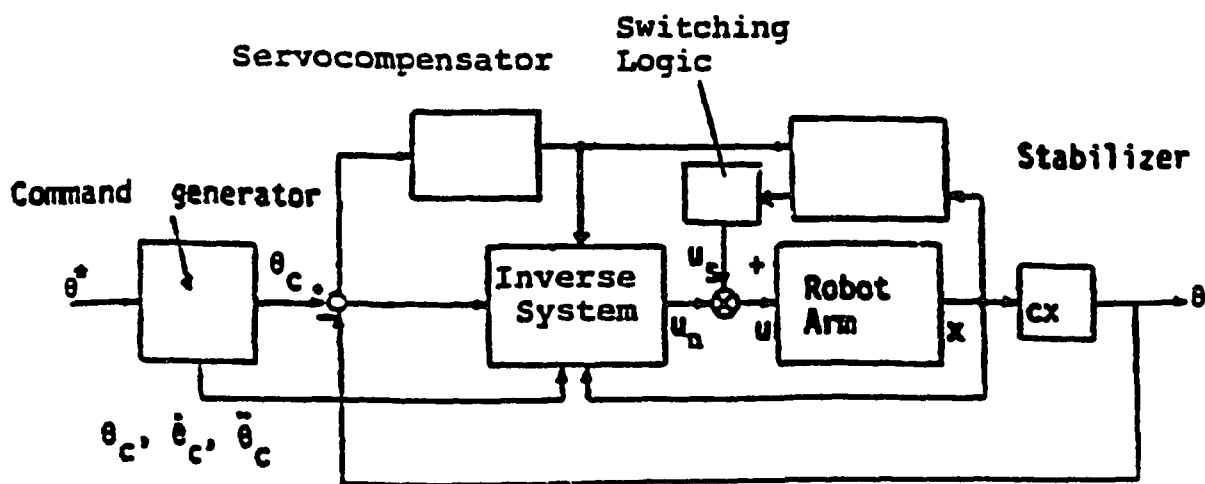


Figure 2

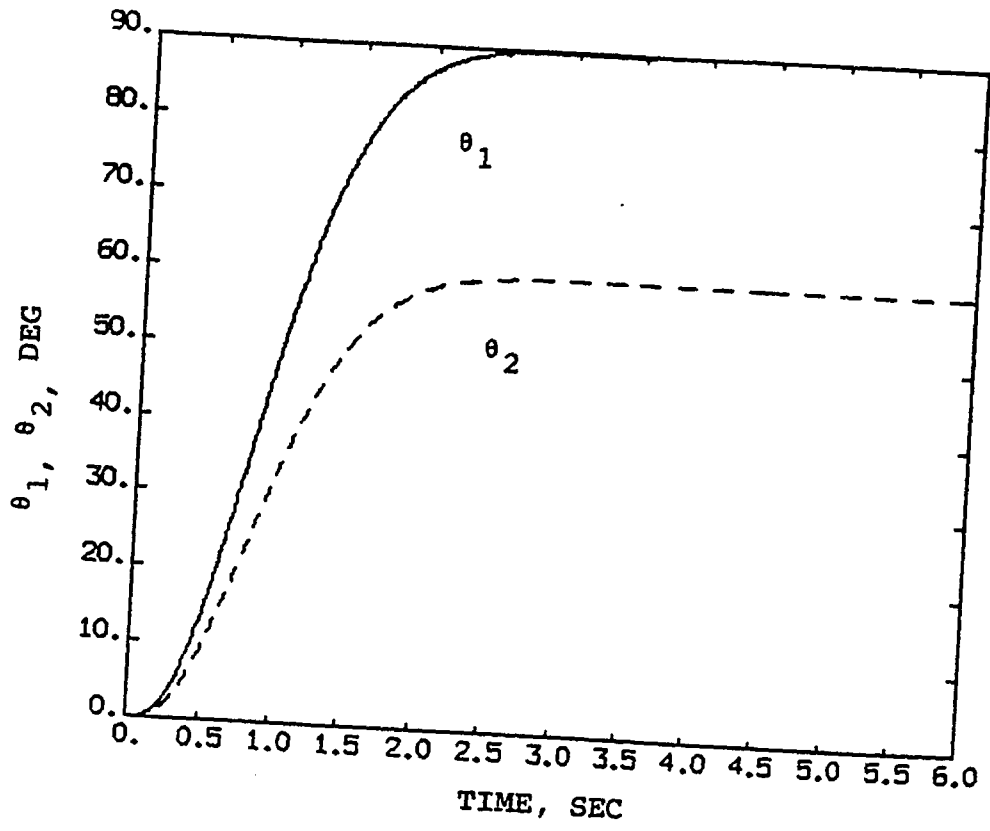


Figure 3(a)

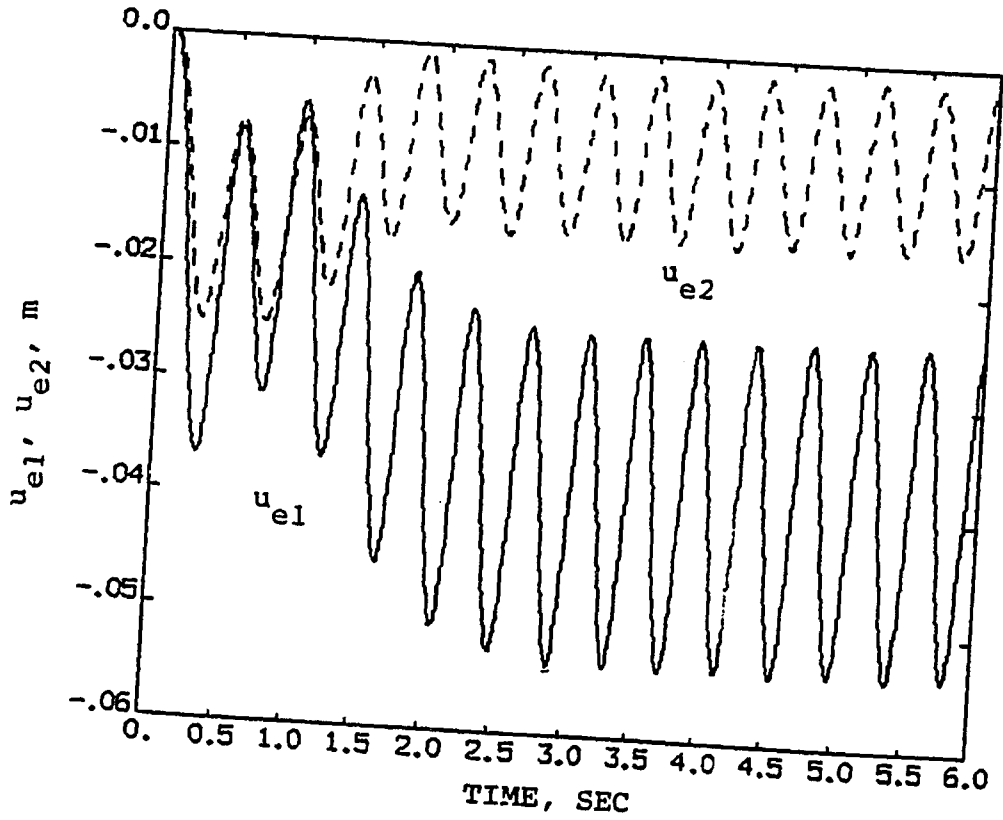


Figure 3(b)

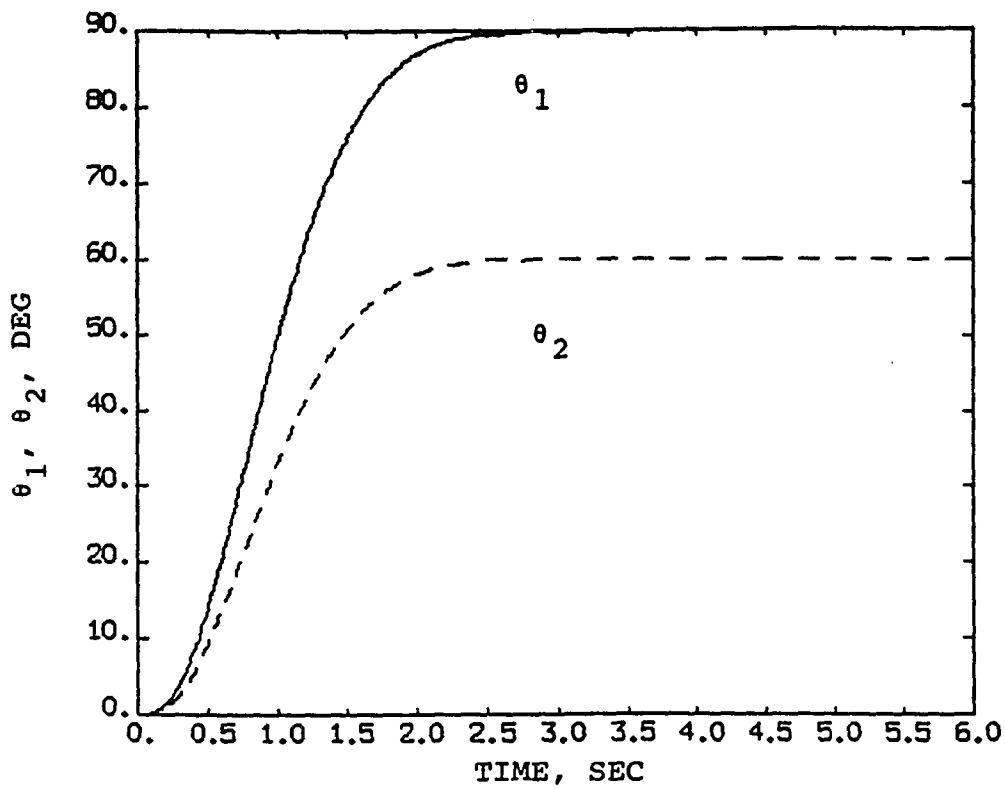


Figure 4(a)

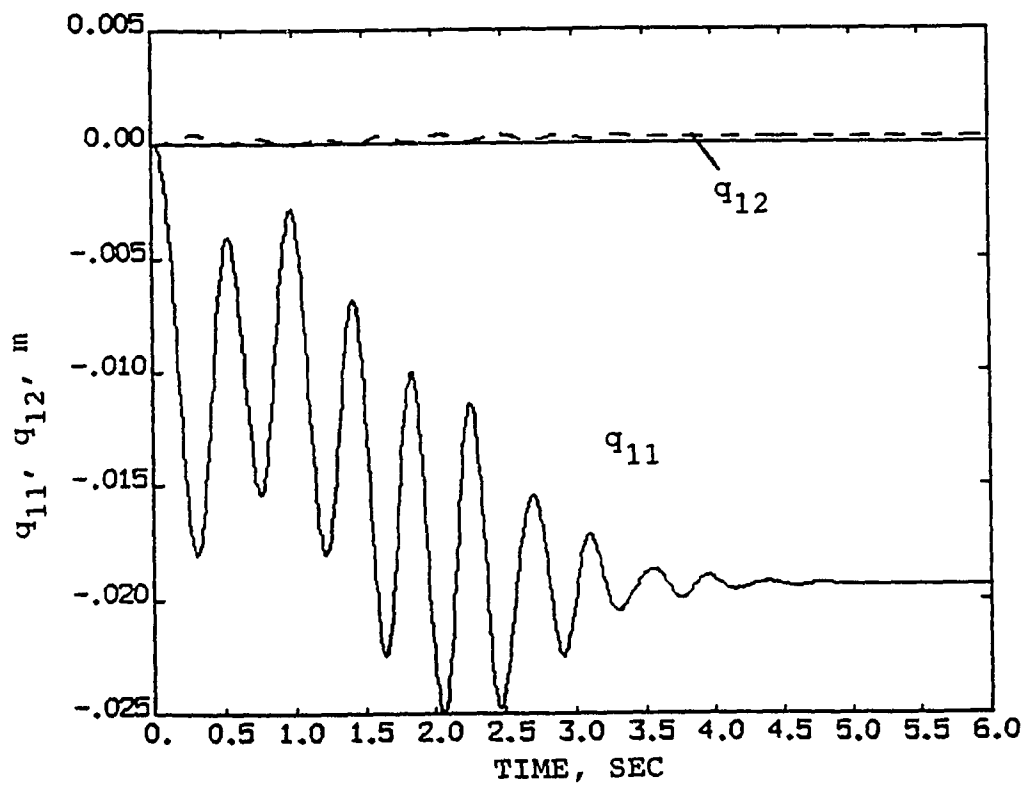


Figure 4(b)

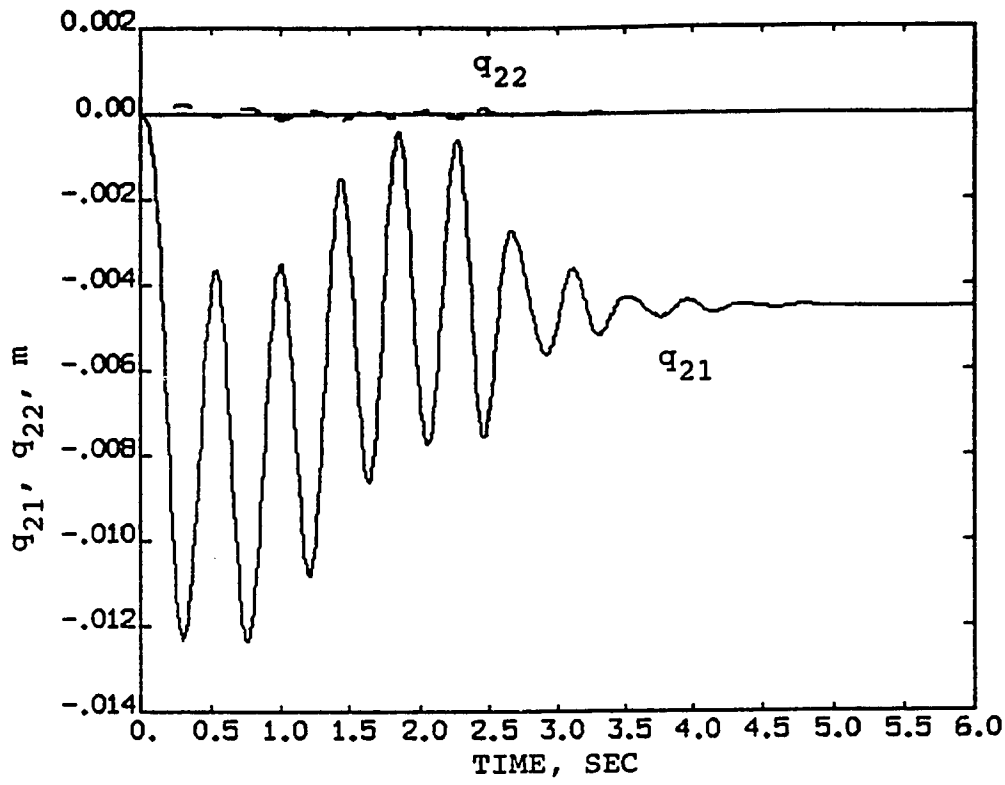


Figure 4(c)

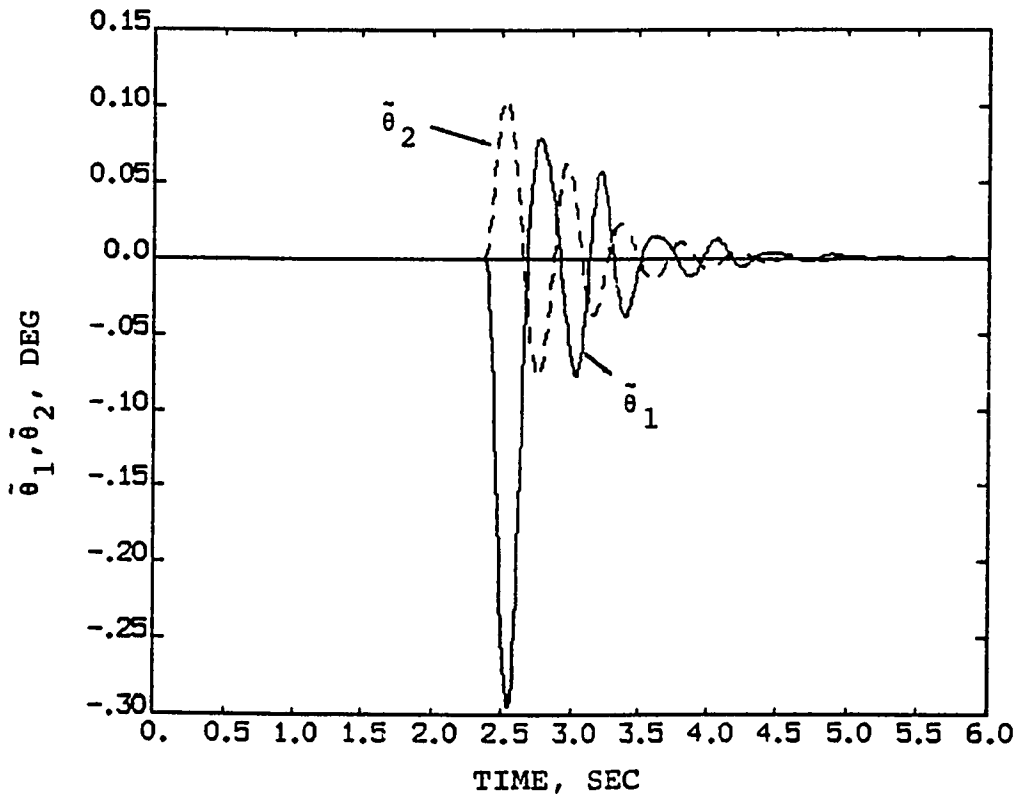


Figure 4(d)

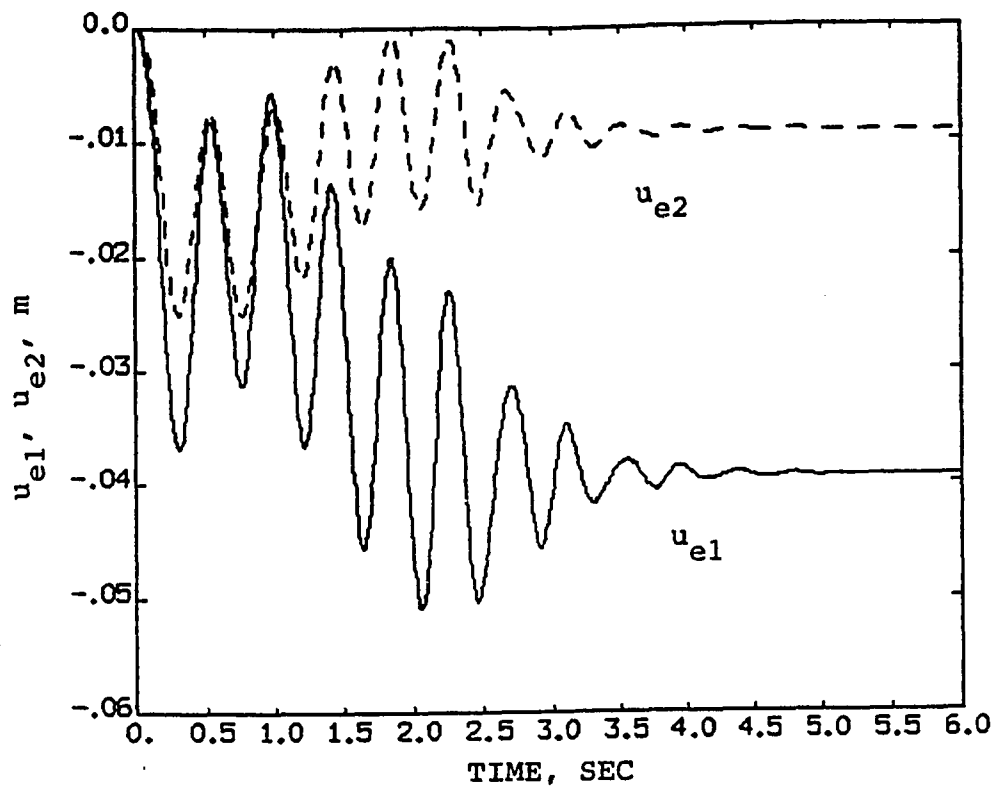


Figure 4(e)

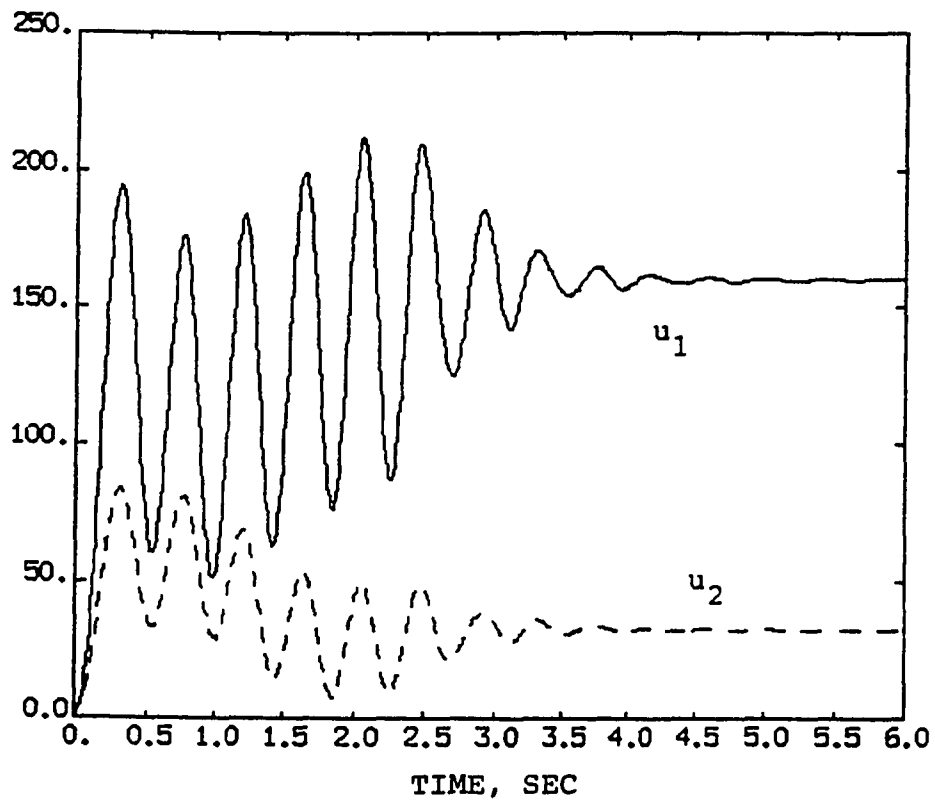


Figure 4(f)

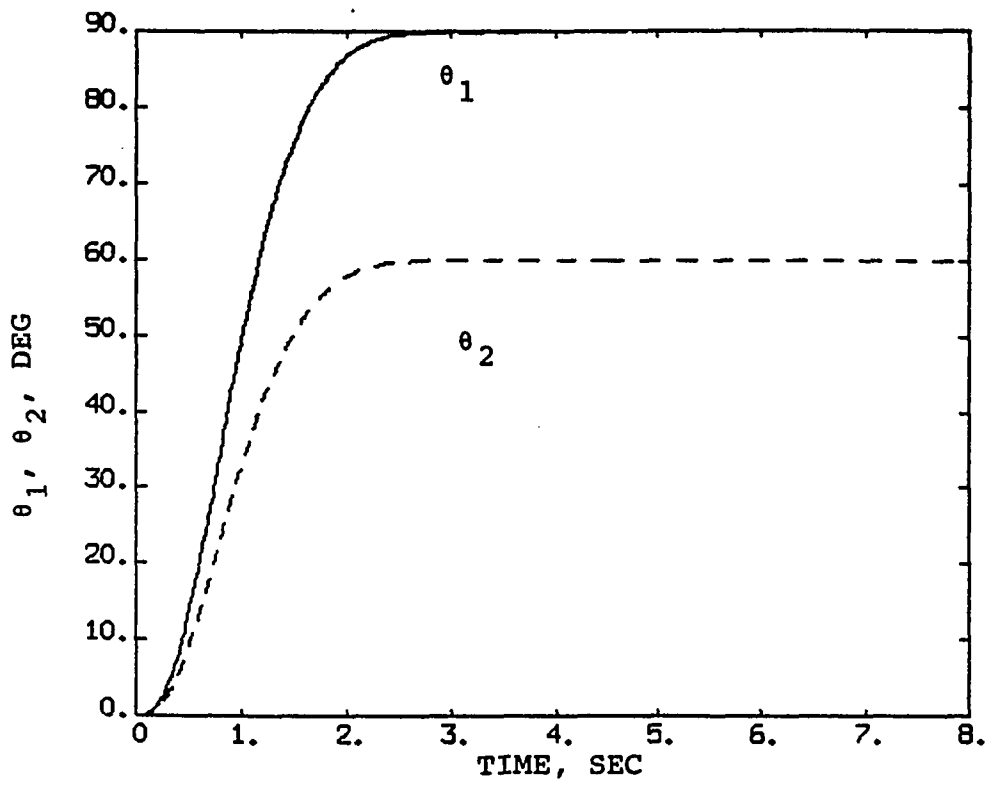


Figure 5(a)

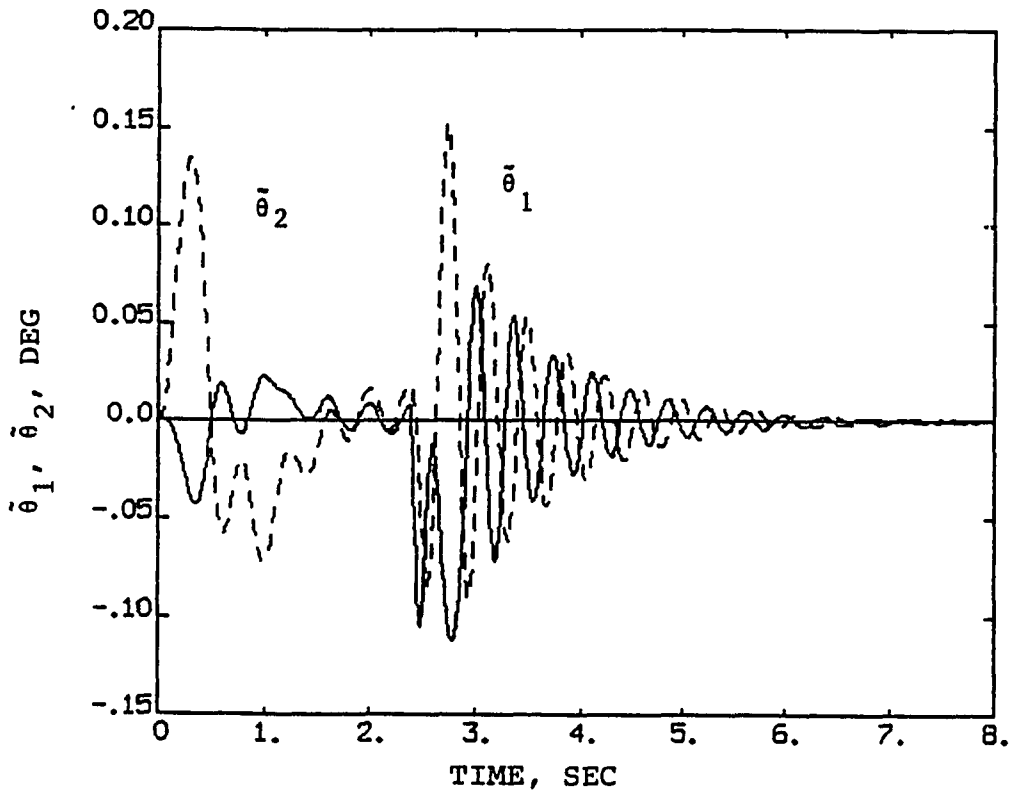


Figure 5(b)

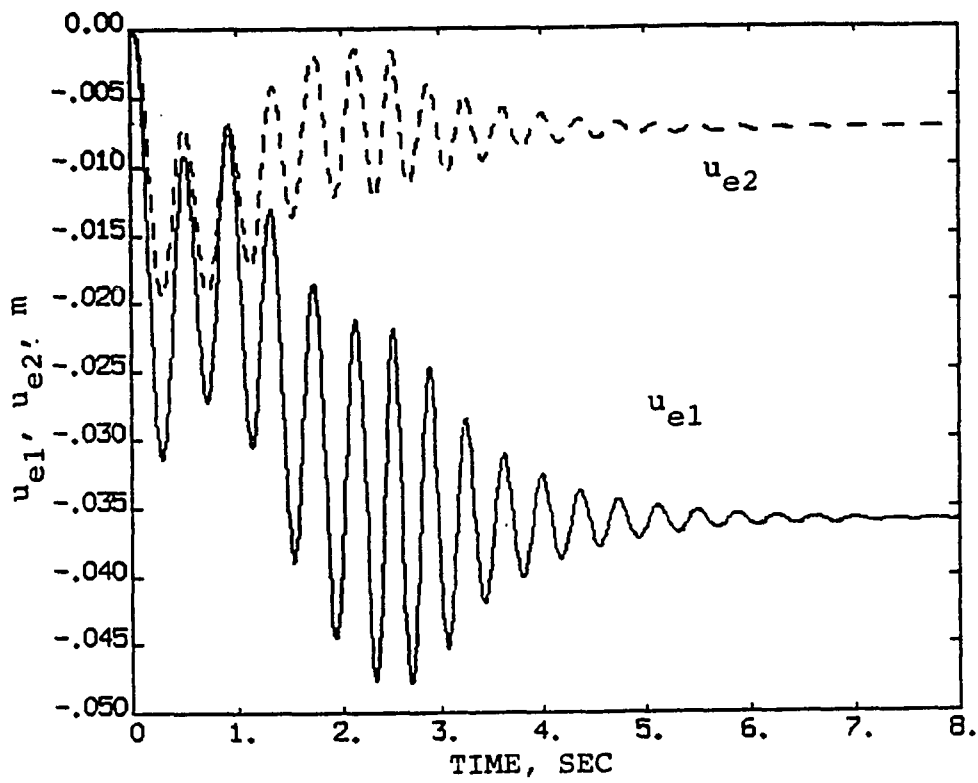


Figure 5(c)

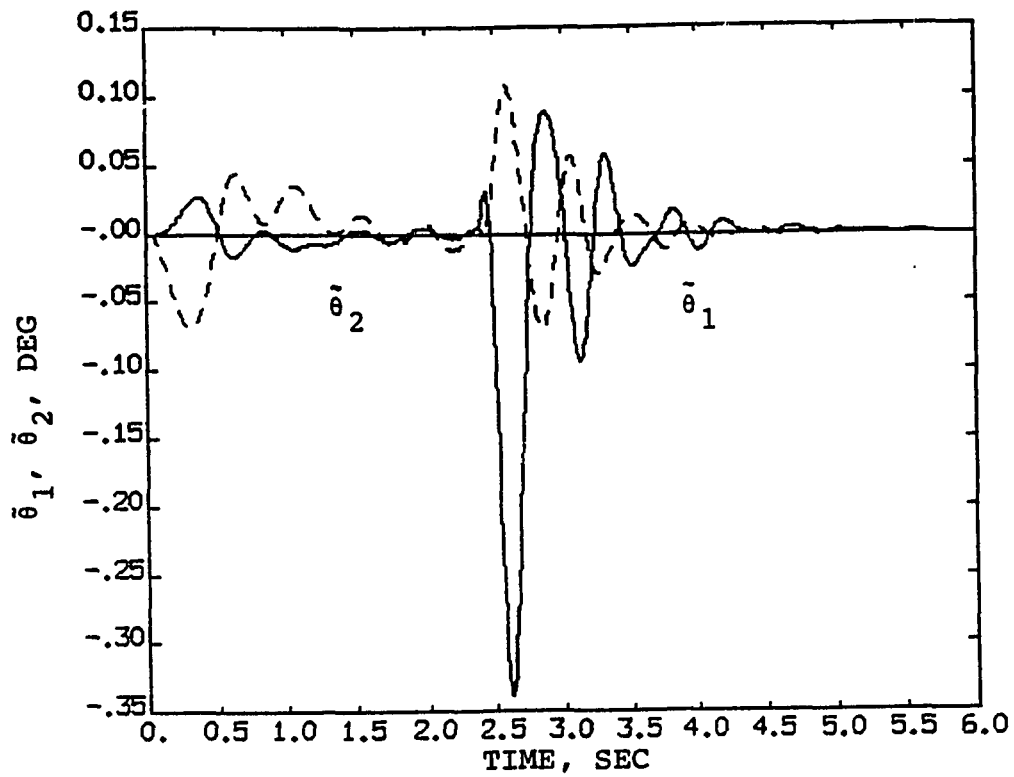


Figure 6(a)

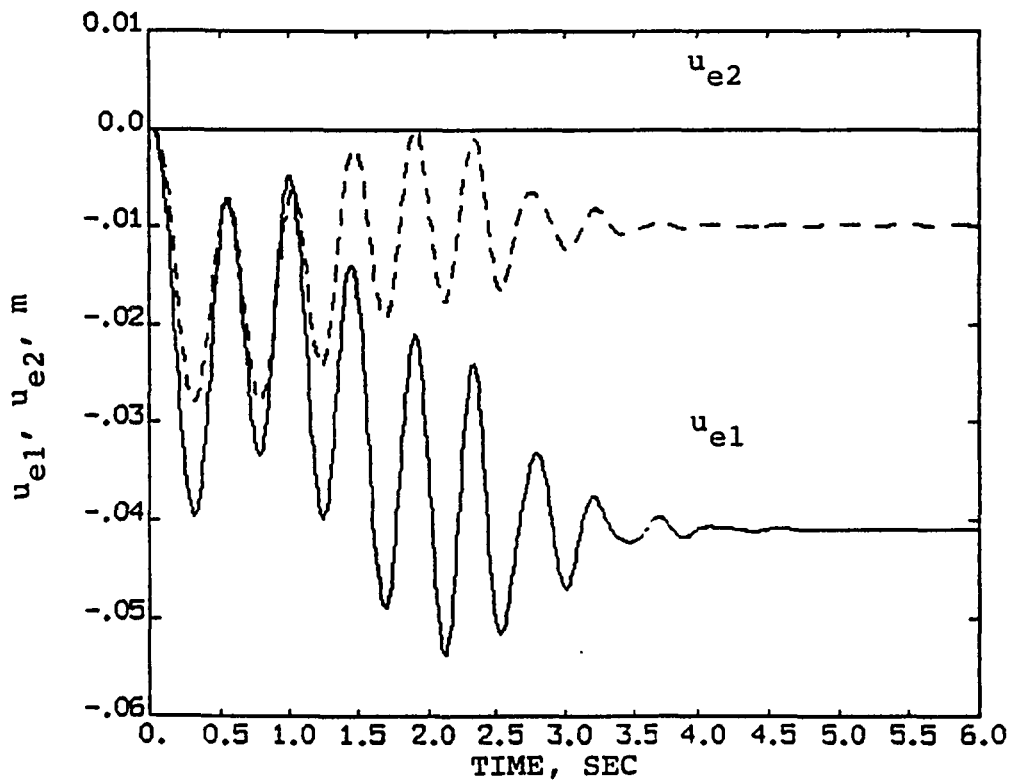


Figure 6(b)

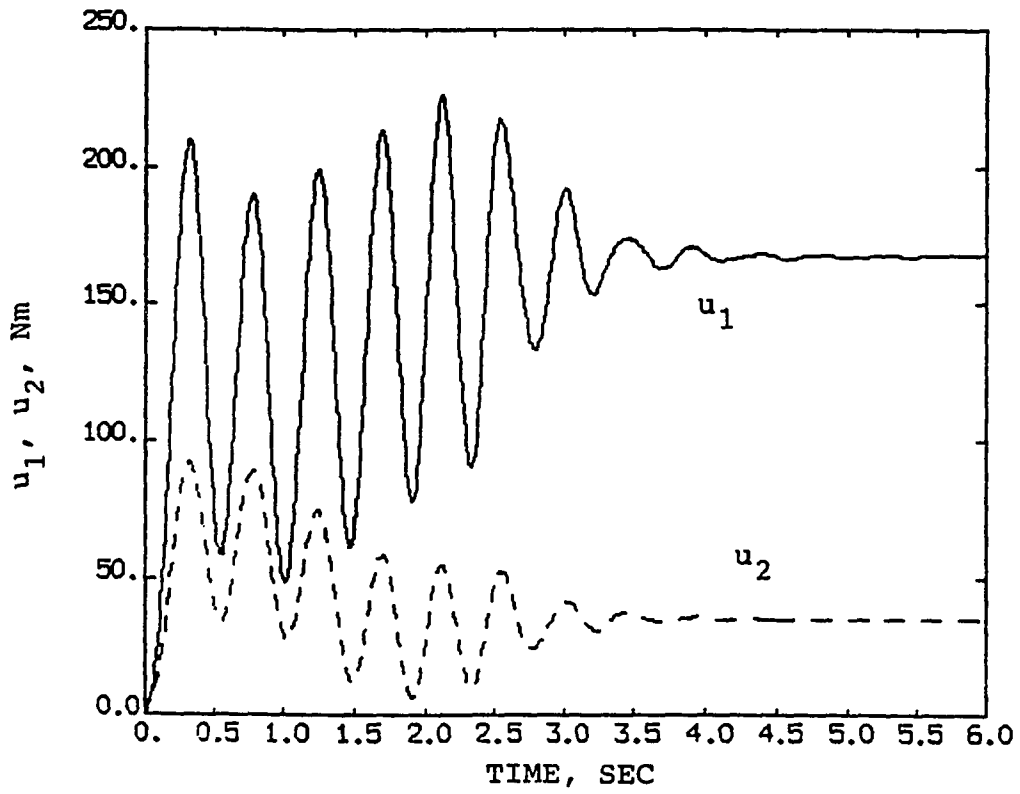


Figure 6(c)

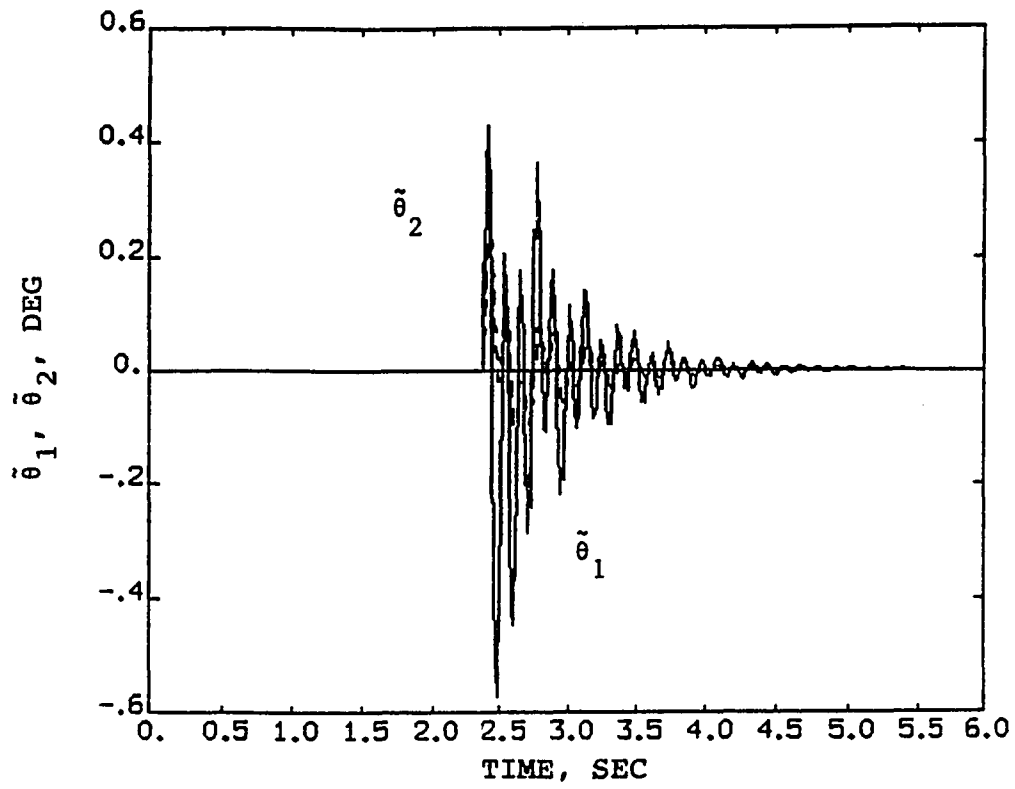


Figure 7(a)

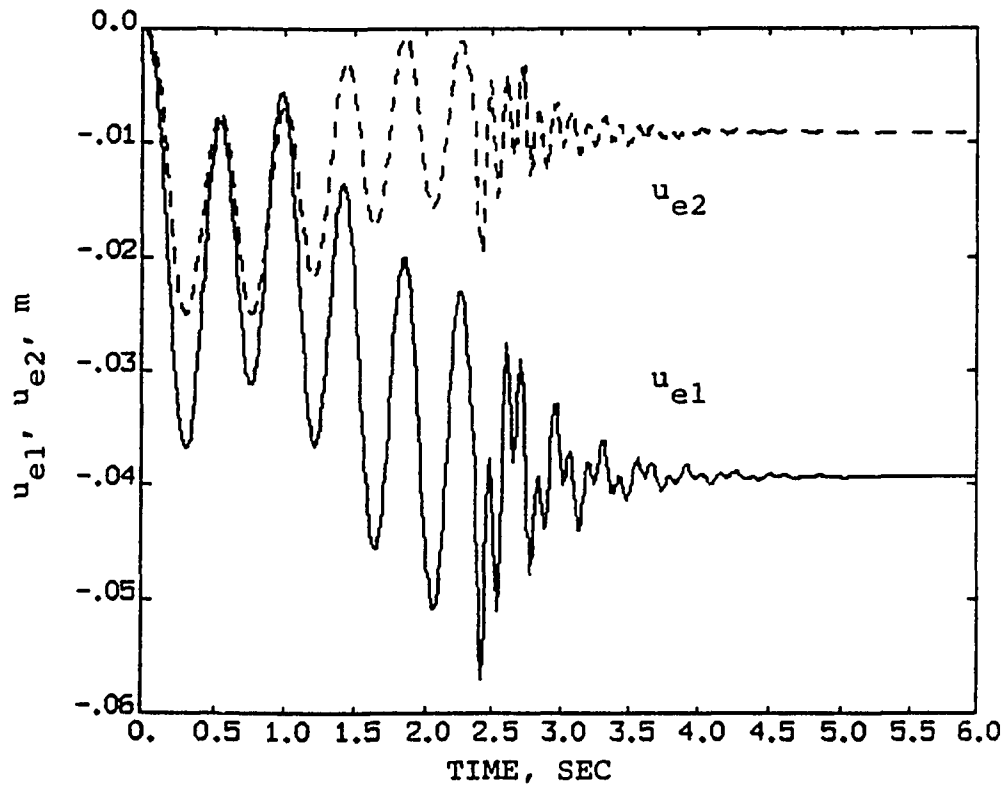


Figure 7(b)

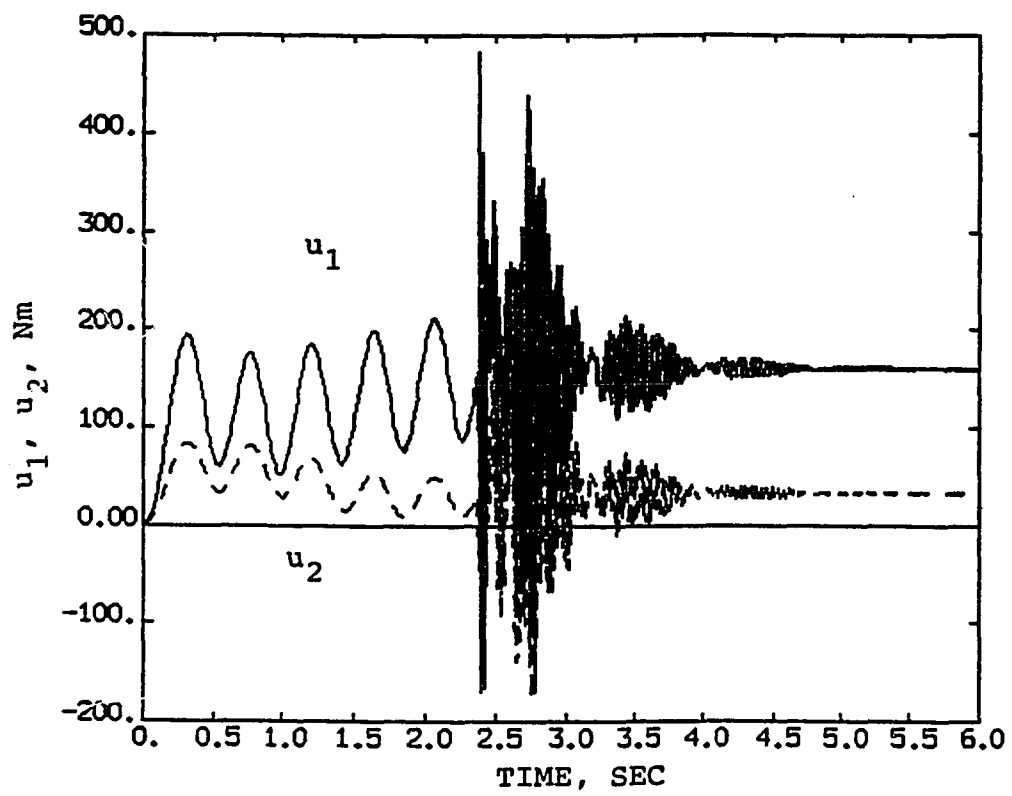


Figure 7(c)

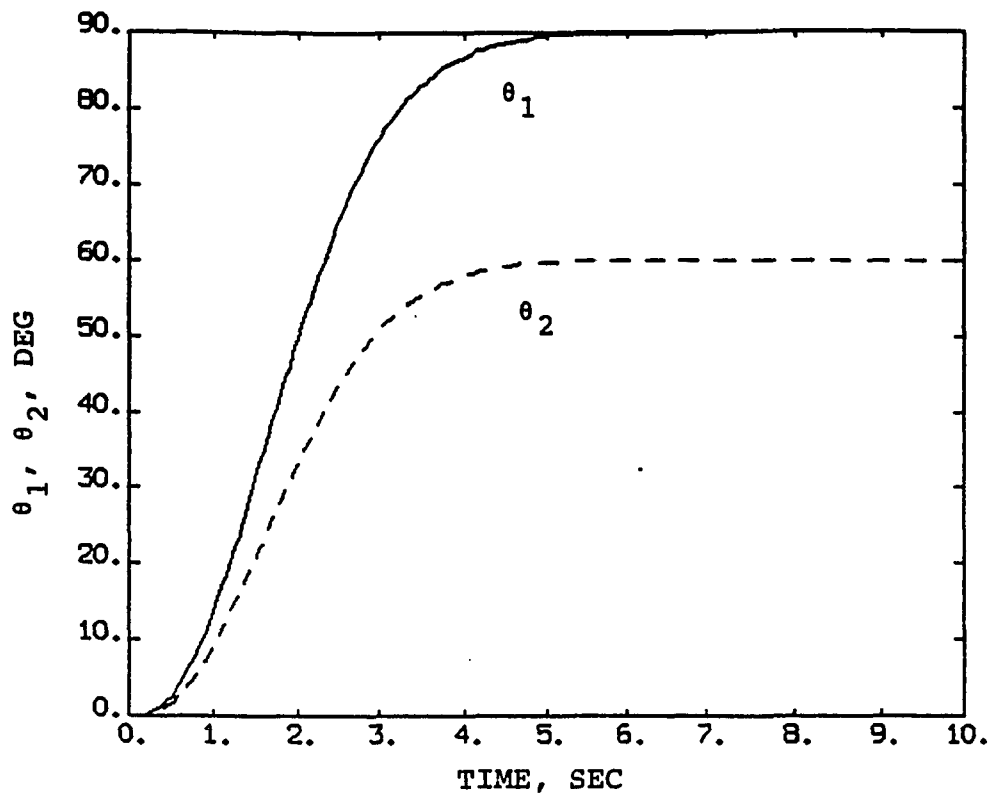


Figure 8(a)

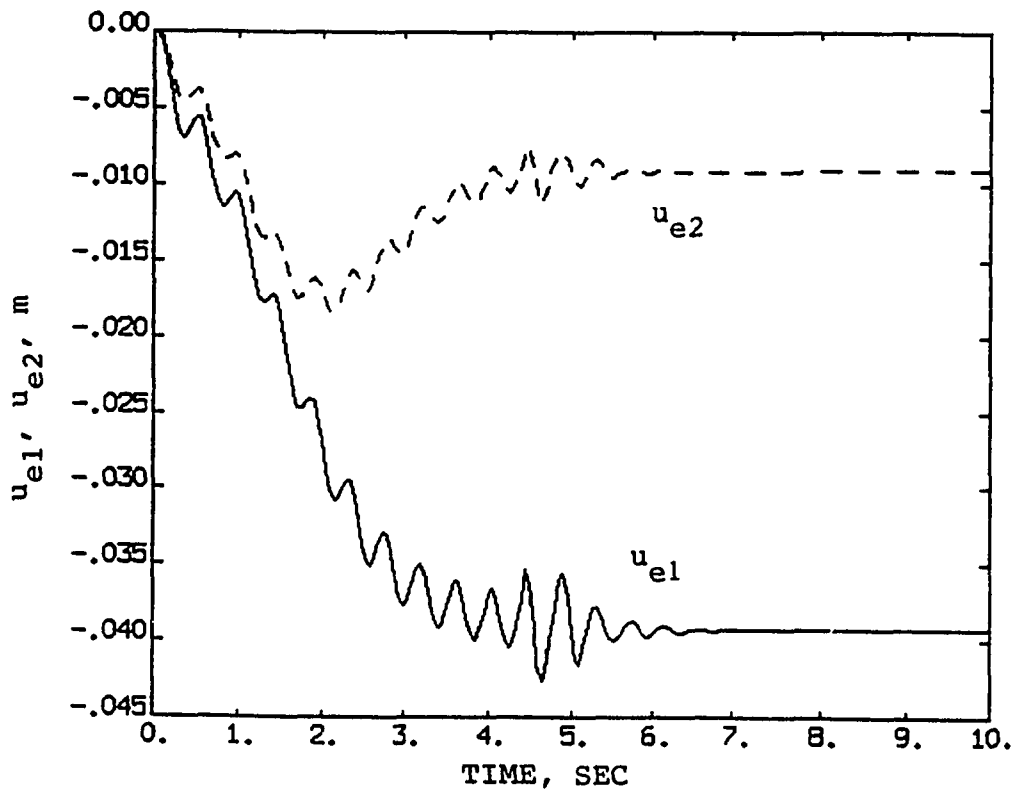


Figure 8(b)

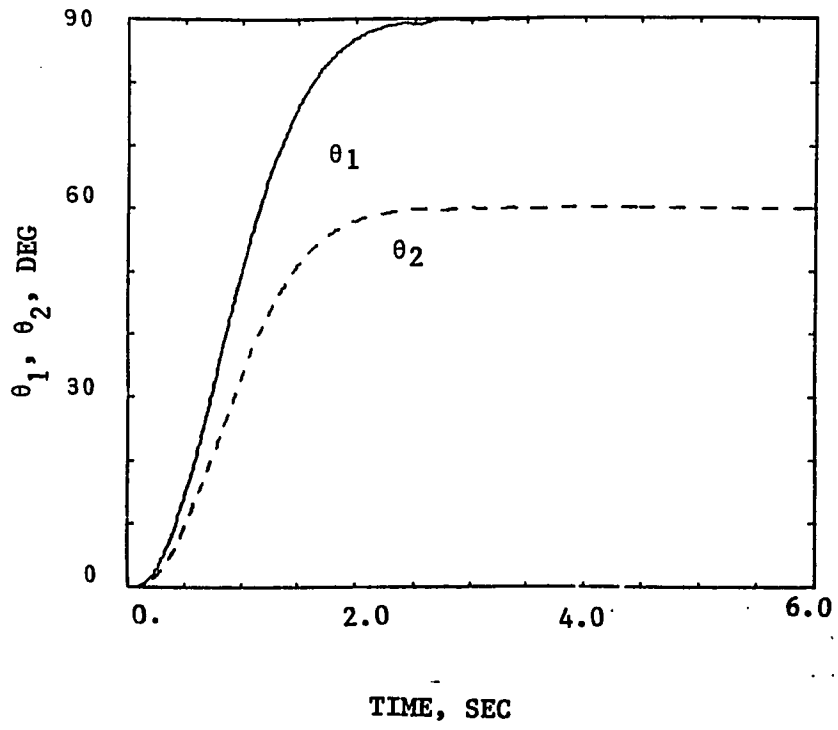


Figure 9(a)

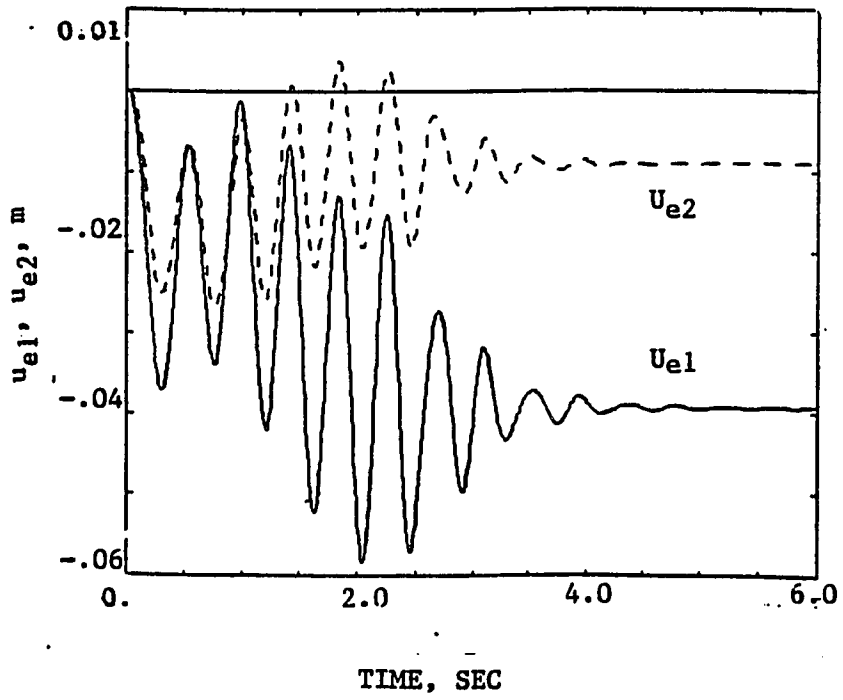


Figure 9(b)

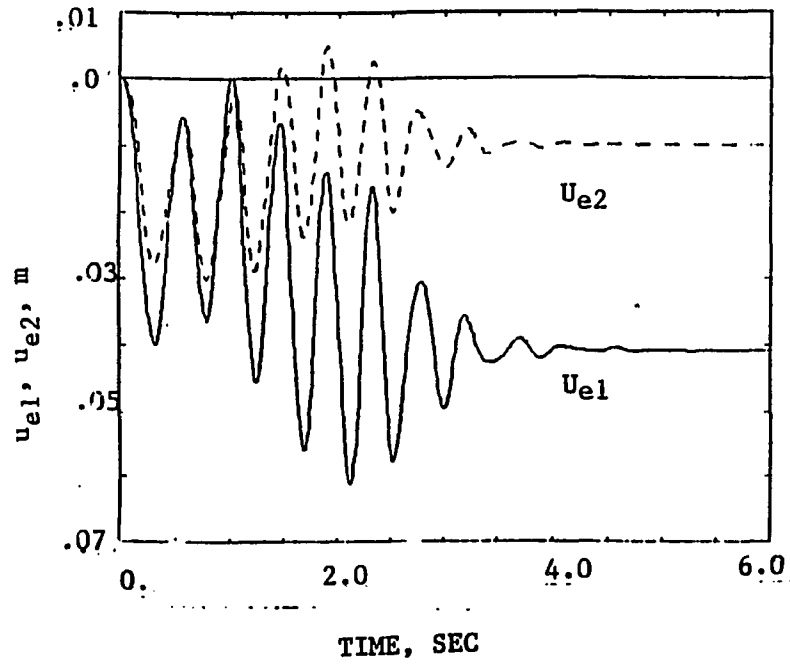


Figure 10(a)

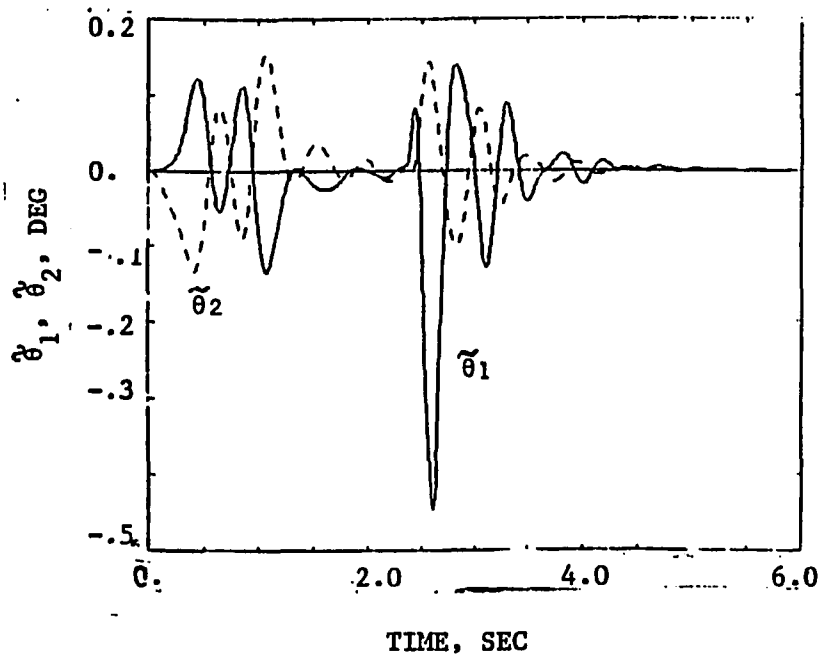


Figure 10(b)

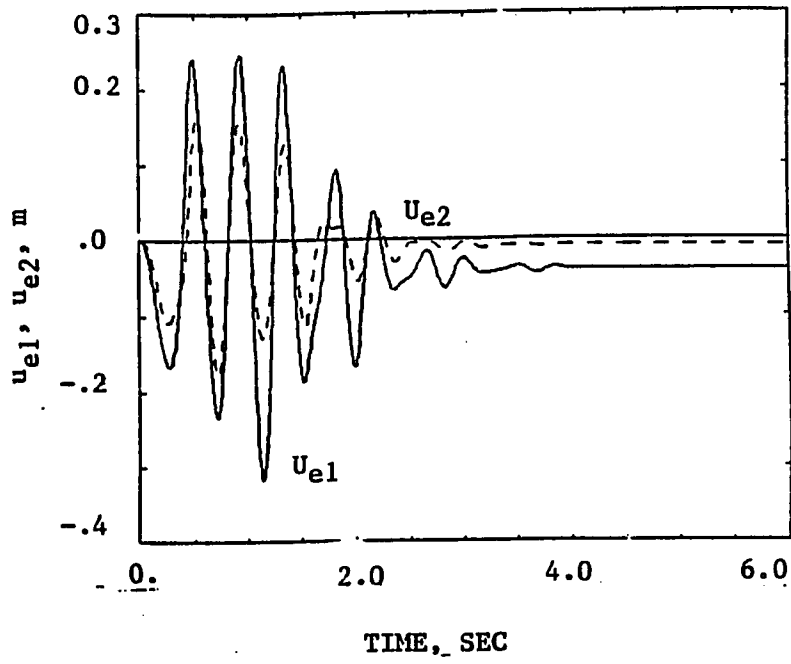


Figure 11(a)

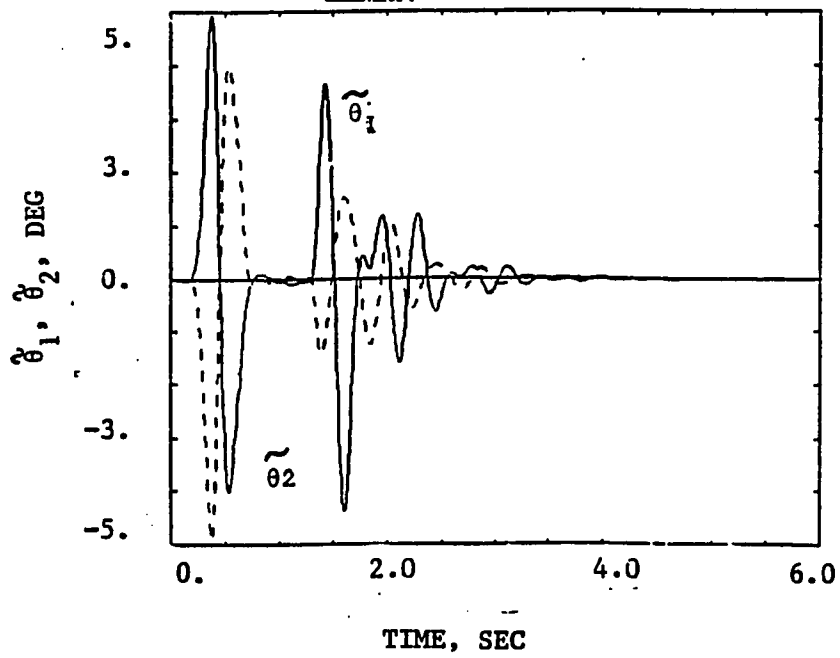


Figure 11(b)

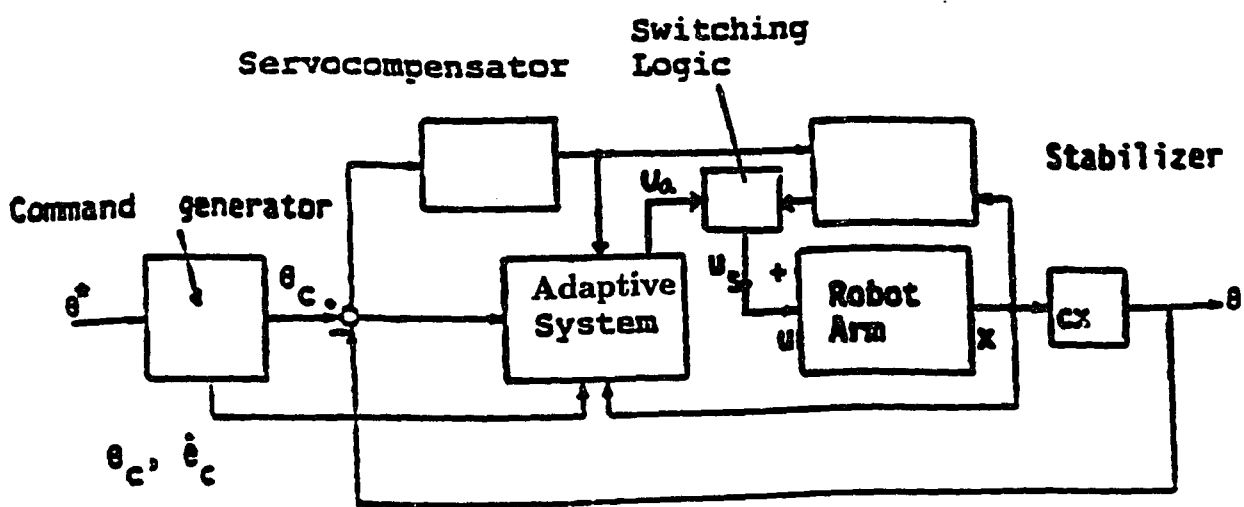


Figure 12

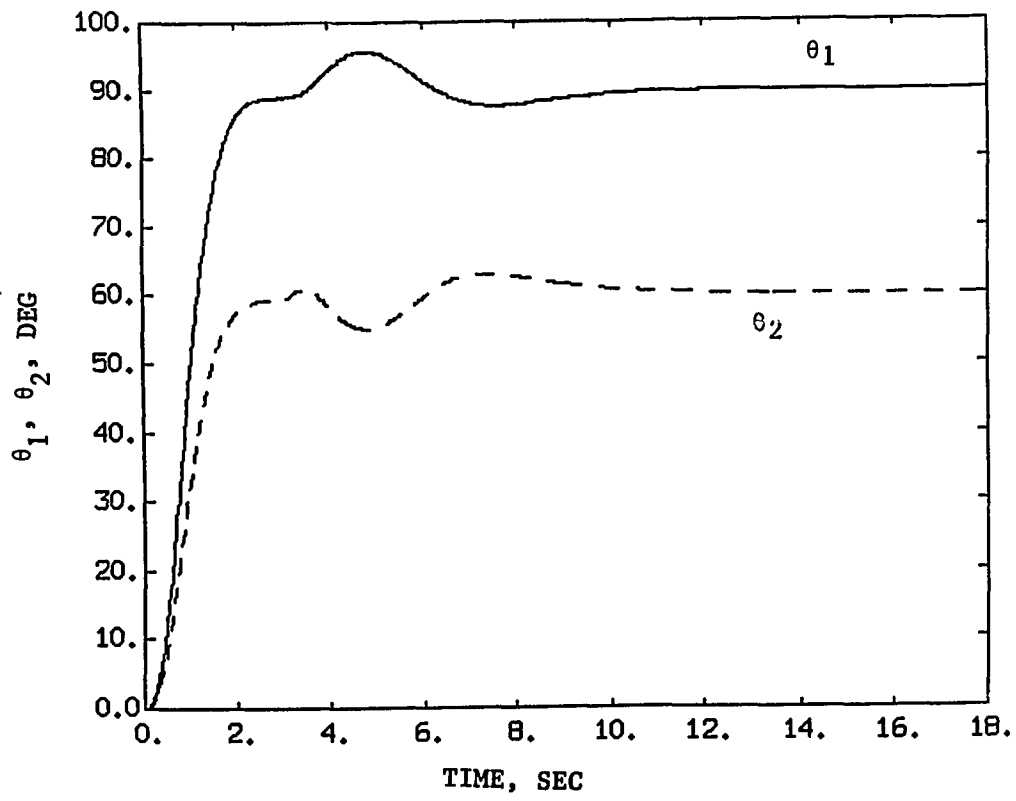


Figure 13(a)

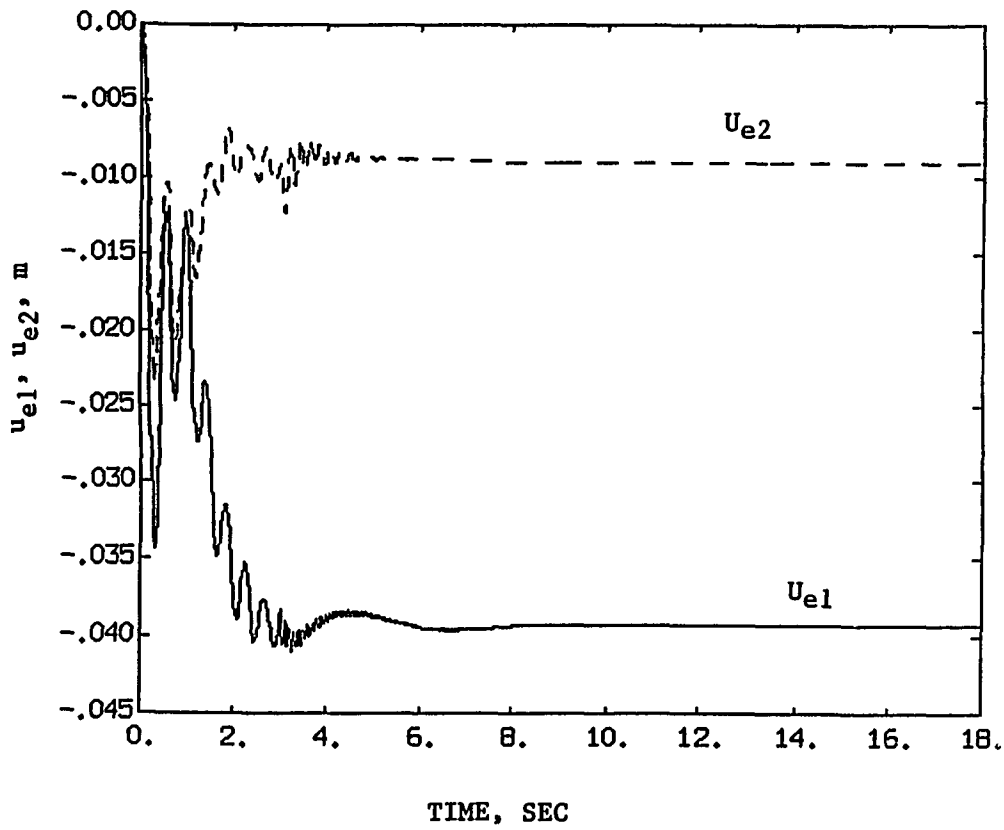


Figure 13(b)

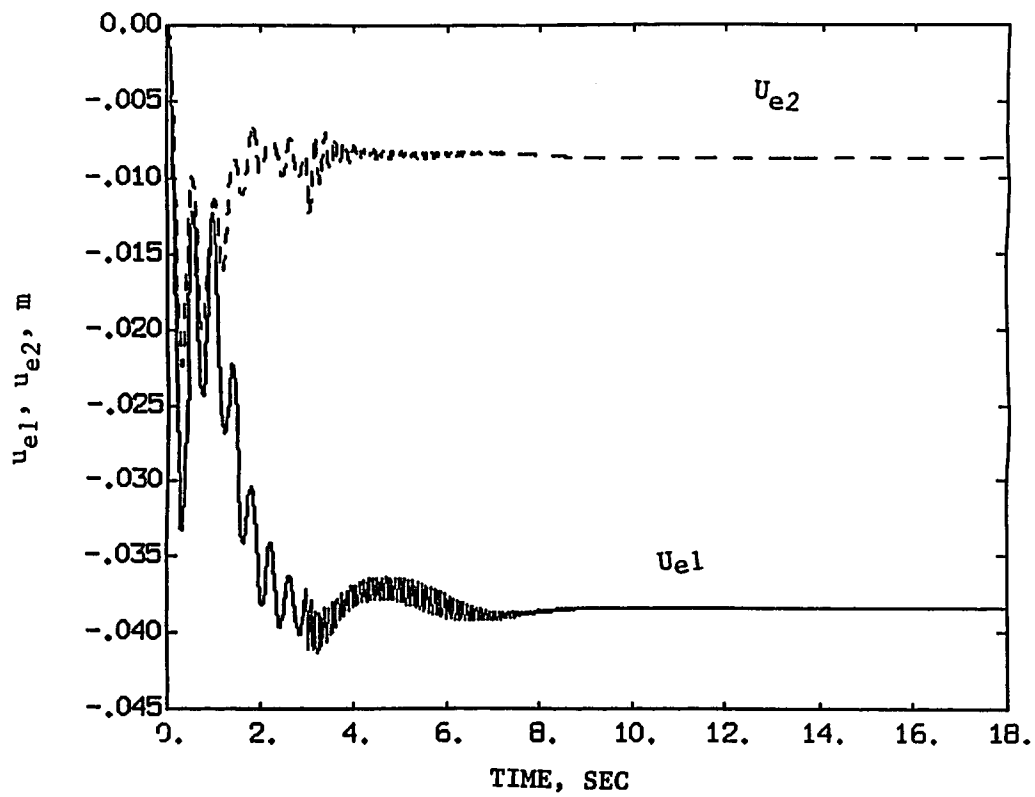


Figure 14(a)

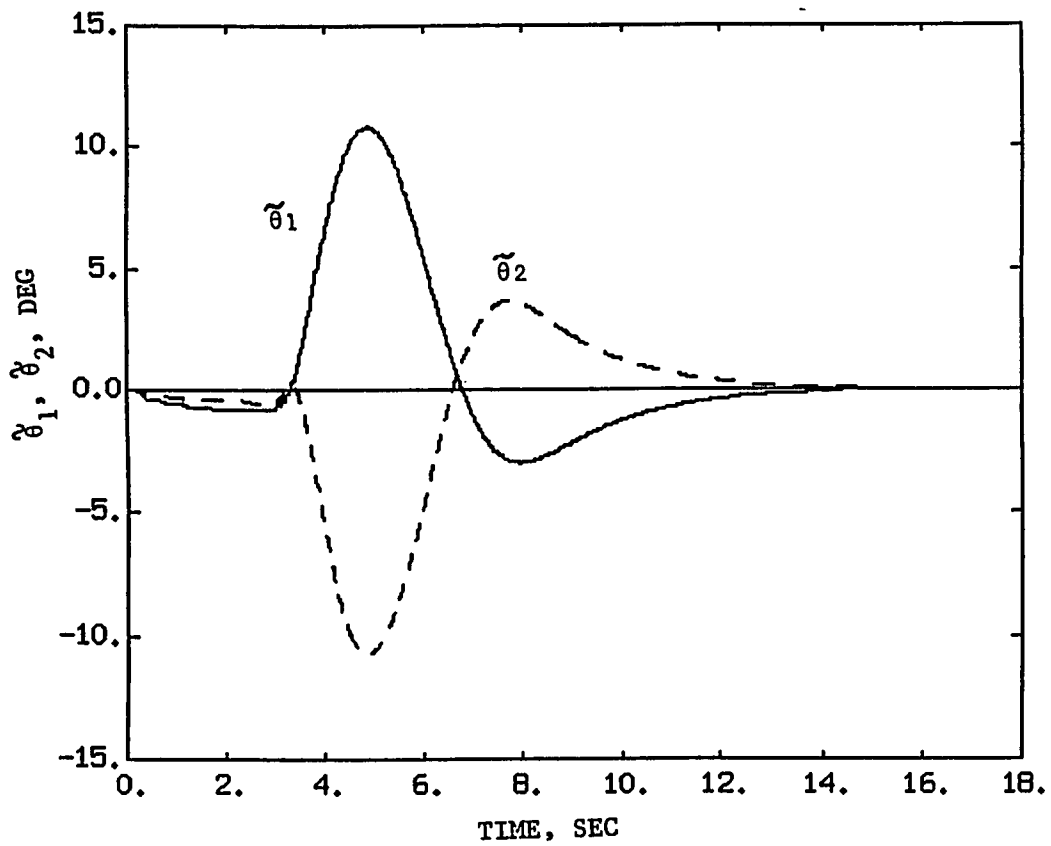


Figure 14(b)

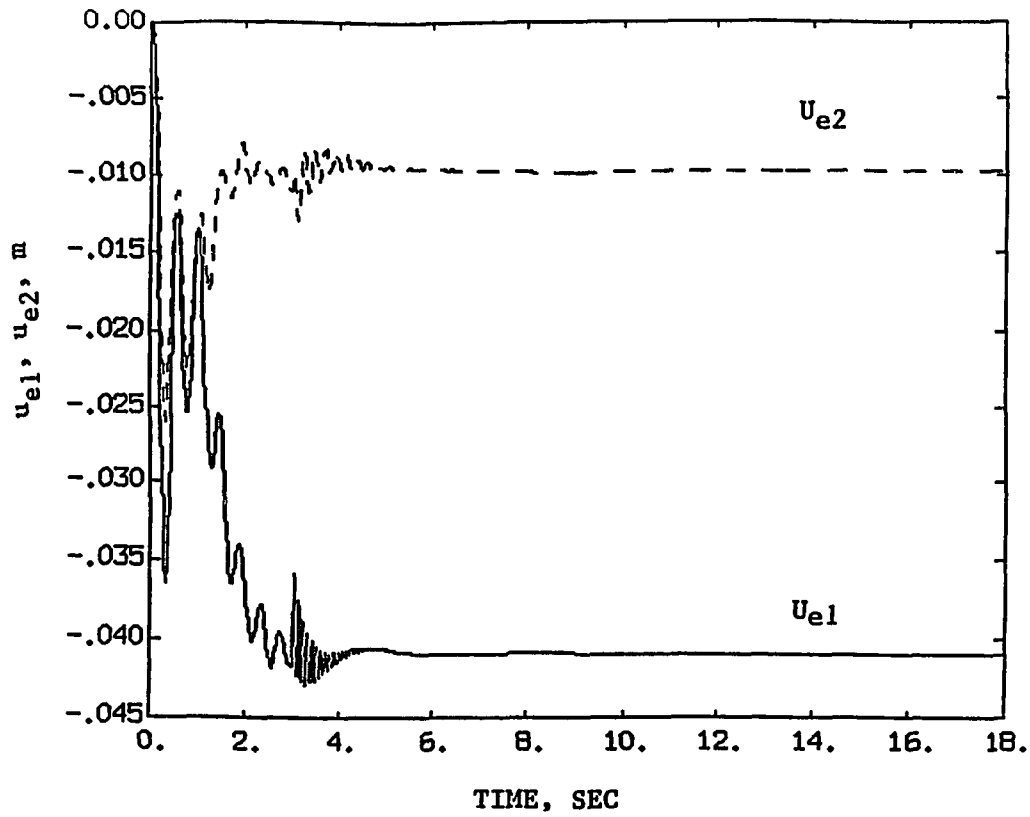


Figure 15(a)

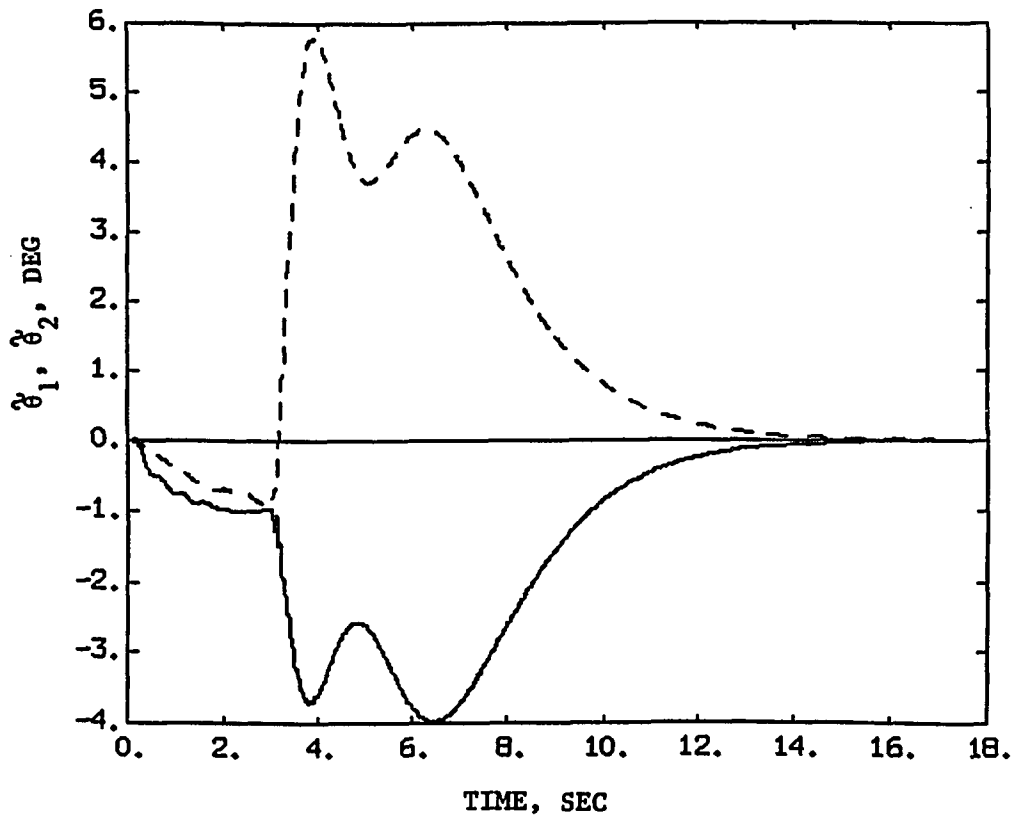


Figure 15(b)